

Fermi National Accelerator Laboratory

FERMILAB-Pub-87/91-A
June 1987

David N. Schramm

NASA/Fermilab Astrophysics Group
Fermi National Accelerator Laboratory
P.O. Box 500
Batavia, IL 60510

and

Department of Physics and Astronomy and Astrophysics
The University of Chicago
Chicago, IL 60637

Submitted for publication in **Comments on Nuclear and Particle Physics.**

NEUTRINOS FROM SUPERNOVA 1987A

David N. Schramm

The University of Chicago,
Fermi National Accelerator Laboratory, and
Max Planck Institut für Physik und Astrophysik

ABSTRACT

This comment will focus on the neutrinos from SN 1987A. Experimental groups from IMB, Kamiokanda, Mount Blanc, and Baksan have reported the detection of neutrinos from the supernova in the Large Magellanic Cloud. The pre-supernova star was a massive object, 15–20 M_{\odot} which was blue, not red. This comment summarizes how such a star can explode and produce neutrinos. Not only did this detection establish extra-solar system neutrino astronomy, but it also constrained the properties of neutrinos. The model-independent constraints on neutrino properties are presented, as well as those conclusions which are more dependent on the details of the supernova model. Specifically, it is argued that $\gamma\tau_{\bar{\nu}_e} > 1.6 \times 10^5$ yr, that $m_{\bar{\nu}_e} < 30$ eV, and that the number of neutrino families, $N_{\nu} \lesssim 7$ and that axions are severely constrained. These limits can be tightened if assumptions are made about the expected nature of the neutrino burst. Any claim of a finite ν mass is very model-dependent. It is shown that the Kamioka-IMB neutrino burst experimentally implies an event with about 2 to 4×10^{53} ergs emitted in neutrinos and a temperature, $T_{\bar{\nu}_e}$, of between 4 and 4.5 MeV. This event is in excellent agreement with what one would expect from the gravitational core collapse of a massive star. While a couple of the Kamioka events are probably due to electron scattering, the lack of ν_e detection at Homestake's detector partially constrains models which produce significantly more ν_e 's at higher energy than the standard model. A neutrino detection, reported earlier in Mt. Blanc, if real, would imply $\gtrsim 4 \times 10^{54}$ ergs emitted in neutrinos with $\bar{\nu}_e$ temperatures between 0.3 and 1.8 MeV. The lack of simultaneous detection by Kamioka is difficult but not impossible to explain with a low temperature, high luminosity event. However, the high luminosity is difficult to understand on theoretical grounds.

As is now well known, on February 23, 1987 light *and neutrinos* from a supernova explosion in the Large Magellanic Cloud (LMC) first reached Earth. Since the LMC is 50 kpc away (a satellite of our Milky Way Galaxy) this was the closest visual supernova since Kepler observed one almost 400 years ago.

For SN 1987a, neutrinos were detected by the Kamioka¹, IMB², Mt. Blanc³, and Baksan⁴ detectors, making this *the birth of extra-solar system neutrino astronomy*. Almost every astrophysicist with any knowledge of neutrinos upon hearing of a supernova in LMC made the trivial, back-of-the-envelope calculation that showed that some existing neutrino detectors should expect to see a signal, and indeed signals were detected. Such a neutrino detection can immediately provide important constraints on neutrino properties. The length of travel automatically tell us that $\gamma\tau_{\bar{\nu}_e} > 1.7 \times 10^5$ yr, where γ is the relativistic factor and $\tau_{\bar{\nu}_e}$ is the anti-electron neutrino lifetime. (Note that the detectors were mainly sensitive to $\bar{\nu}_e$, thus most constraints are on $\bar{\nu}_e$.) Also, the duration of the detected neutrino bursts puts an upper limit on the mass, $m_{\bar{\nu}_e}$. It is only an upper limit since the spreading in time of the neutrino signal might also be due to the intrinsic duration of the neutrino emission. More papers have been written on m_ν from SN 1987a than neutrinos detected. The major difference between the papers is what assumption is made about the intrinsic spread of the emitted burst versus what part of the observed burst might be due to finite mass induced spreading. Among other things, this paper will go through the basic arguments and show that without making specific model assumptions, all that can be safely said is, $m_{\bar{\nu}_e} \lesssim 30$ eV, which is not as restrictive as limits from tritium decay. It will also be shown that since a stellar collapse presumably produces all types of neutrinos, the detection of $\bar{\nu}_e$'s argues that there are not too many other types ($N_\nu \lesssim 7$), or otherwise the share at binding energy radiated as $\bar{\nu}_e$'s would reduce the flux to unobservable levels. This argument also constrains axion properties.

A major problem regarding neutrinos from SN 1987a is that while one burst was detected definitively by Kamioka and IMB, with concordant signals also found at Baksan and Mt. Blanc, another burst was reported earlier by Mt. Blanc and not definitely seen by the other detectors. While it is difficult to understand how Mt. Blanc could have seen something without Kamioka (a much larger detector with *almost* the same energy threshold) seeing it too. As emphasized by de Rujula²⁵, it is not impossible that a low temperature $\bar{\nu}_e$ burst could replicate the observations, but such a burst would require far more energy than any model yields.

NEUTRINO EXPECTATIONS

For over 20 years, it has been known that the gravitational collapse events thought to be associated with Type II supernovae and neutron star or black hole formation are copious producers of neutrinos. In fact, the major form of energy transport in these objects comes from neutrino interactions. It has long been predicted that the neutrino fluxes produced by these events would be high enough that if an event occurred within the galaxy, it could be detected

It has been well established in the models of Arnett⁵ and Weaver et al.⁶ that massive stars with $M \gtrsim 8M_\odot$ evolve to an onion-skin configuration with a dense central iron core of about the Chandrasekhar mass surrounded by burning layers of silicon, oxygen, neon, carbon, helium, and hydrogen. Collapse inevitably occurs when no further nuclear energy can be generated in the core. While for Pop I abundances such stars are usually red

giants when they collapse and explode, for the low metallicity of the LMC it is possible for 15–20 M_{\odot} stars to undergo core collapse before moving all the way to the red³⁸. It is also possible for an evolved red star to shift to the blue before exploding⁵³. A more compact blue envelope would naturally lead to higher velocities and lower luminosities than with extended red envelopes. It would also result in hours rather than days between core collapse and the light outburst. A supernova display is seen if the star's envelope can be ejected. To have such an ejection occur while allowing the core to collapse to a neutron star or black hole depends on the detailed physics of the core's equation of state and the neutrino transport of energy and momentum, as well as the hydrodynamics.

Bethe and Brown⁷ and Baron et al.⁸ have argued that, provided the equation of state of matter above nuclear density is very soft, stars in the mass range $10 \leq M \leq 16M_{\odot}$ may explode due to the prompt exit of the shock wave formed after the core bounces upon reaching supra-nuclear density. For stars with $16 \leq M \leq 80M_{\odot}$, the shock wave stalls on its exit from the core and becomes an accretion shock. Wilson et al.⁹ have shown that such stars will eventually (~ 1 second later) eject their envelope as a result of neutrino heating in the region above the neutrinosphere and below the shock. (The delayed ejection can also occur in the lower mass collapses if the initial bounce does not produce an explosion.) In fact, if collapse to a black hole is delayed by about a second after bounce, the neutrino spectra and mass ejection should not be affected by the later formation of the black hole. Obviously the above scenarios are sensitive to the stiffness of the core equation of state which is still poorly known at and above nuclear mass densities.

As was first emphasized by Arnett and Schramm¹⁰, the ejecta have a composition which fits well with the observed 'cosmic' abundances for the bulk of the heavy elements.

Regardless of the details of collapse, bounce, and explosion, it is clear that to form a neutron star the binding energy, $\epsilon_B \approx 2 \times 10^{53}$ ergs must be released. The total light and kinetic energy of a supernova outburst is about 10^{51} ergs. Thus, the difference must come out in some invisible form, either neutrinos or gravitational waves. It has been shown¹¹ that gravitational radiation can at most carry out 1% of the binding energy for reasonable collapses because neutrino radiation damps out the non-sphericity of the collapse (see Kazanas and Schramm^{12,13}). Thus, the bulk ($\gtrsim 99\%$) of the binding energy comes off in the form of neutrinos.

It is also well established¹⁴ that for densities greater than about 2×10^{11} g/cm³, the core is no longer transparent to neutrinos. Thus, as Mazurek¹⁵ first established, the inner core has its neutrinos degenerate and in equilibrium with the matter. For electron neutrinos, the 'neutrinosphere' has a temperature such that the average neutrino energy is around 10 MeV. This was established once it was realized that the collapsing iron core mass is $\sim 1.4M_{\odot}$, due to the role of the Chandrasekhar mass in the pre-supernova evolution. Since the μ and τ neutrinos and their antiparticles only interact at these temperatures via the neutral, rather than the charged, current weak interaction, their neutrinosphere is deeper within the core. Therefore, their spectra are hotter than either the electron neutrino and antineutrino spectra.

The average emitted neutrino energy is actually quite well determined for the peak of the neutrino distribution and is very insensitive to model parameters. The peak occurs at the highest temperature for which neutrinos can still free stream out of the star; that is, where the neutrino mean free path, $[n\langle\sigma\rangle]^{-1}$, is comparable to the size of the core, R .

This can be expressed as

$$R \simeq 1/n\langle\sigma\rangle \quad (1)$$

where n is the number density $= \rho/m_n$, ρ being the mass density and m_n the nucleon mass. Collapsing stars are well described by adiabatic physics. Thus density and temperature are related as

$$\rho = \rho_0(T/T_0)^3 \quad (2)$$

For a Fermi distribution the average energy $\langle E_\nu \rangle = 3.15T_\nu$ (using T in energy units). The effective neutrino cross section in stars¹⁴ can be expressed as

$$\langle\sigma\rangle \approx 1/2\sigma_0\langle E_\nu^2\rangle \approx 12\sigma_0/2T_0^2\left(\frac{T_\nu}{T_0}\right)^2$$

Inserting this into eq. 1 and solving for T

$$\frac{T_{\nu_e}}{T_0} = \left[\frac{2m_n}{R\rho_0 12\sigma_0 T_0}\right]^{1/5} \quad (3)$$

The neutrino temperature, T , varies only as the 1/5 power of the input. Thus, large uncertainties get minimized. [If R is put at its upper limit from the size of the core, then $R \propto 1/T$. The limiting relationship has T proportional to the 1/4 power, which is still quite insensitive.] Using reasonable values $\sigma_0 \simeq 1.7 \times 10^{-44}$ and $\rho_0 = 10^{10}$ gm/cm³ at $T_0 = 1$ MeV, with the characteristic size of the region $R \lesssim 5 \times 10^6$ cm (see models^{5,6}). Then

$$T_{\nu_e} \approx [340]^{1/5} \text{MeV} \simeq 3.2 \text{MeV}$$

or

$$\langle E_\nu \rangle \approx 10 \text{MeV}.$$

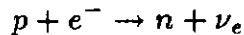
This is in good agreement with detailed numerical results. For $\bar{\nu}_e$'s, T is somewhat higher due to the lower cross section and the evolution of degeneracy effects with time.

It should also be noted that since the interaction cross sections in the star are proportional to the square of the neutrino energy, the lower energy neutrinos can escape from deeper in the star. Thus, the energy distribution of the emitted neutrinos is not a pure thermal distribution at the temperature of the neutrinosphere.

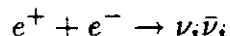
While the general scenario for collapse events is well established, the detailed mechanism for the ejection of the outer envelope in a supernova as the core collapses to form a dense remnant continues to be hotly debated. Therefore, most theorists working on collapse have focused on these details in an attempt to solve the mass-ejection problem. As a result, most of the papers in the literature are concerned with the role played by neutrinos internal to the stellar core, rather than the nature of the fluxes which might be observed by a neutrino detector on earth. In particular, while it has been known since the early 1970's^{16,17} that the average energy of the emitted neutrinos was about 10 MeV, with neutrino luminosities of a few 10^{52} ergs/sec, the detailed nature of the emitted spectra was only recently explored in detail by Mayle, Wilson, and Schramm^{18,19}. Their calculation emphasized the high-energy neutrinos which are easier to detect. The diffusion approximation used in most collapse calculations does not treat the high-energy tail of the spectrum accurately. A large temperature gradient exists in the neutrinospheric region.

For the high-energy neutrinos, the matter's temperature at one optical depth is relatively low compared to the temperature at one optical depth of the mean-energy neutrino. Thus, an appreciable fraction of the high-energy neutrinos originate in the higher temperature region and travel several mean-free paths before exiting the star. Therefore, for neutrinos whose energy is far above the mean energy, the multi-group, flux-limited-diffusion approximation is suspect. To confirm this, Mayle et al. constructed a computer code that integrates the Boltzmann equation more directly. Their results are the models used to illustrate what was anticipated from a stellar-collapse-triggered supernova (see Fig. 1).

In addition to the basic energetic arguments, there is the basic neutronization argument (see ref. 20, and references therein). The collapsing core has $\sim 10^{57}$ protons that are converted to neutrons via



to form a neutron star. Each ν_e , so emitted from the core, carries away on the average 10 MeV, thus around 1.3×10^{52} ergs are emitted by neutronization ν_e 's. this is $\lesssim 10\%$ of the binding energy. The remainder of the neutrinos come from pair processes such as



where $i = e, \mu, \text{ or } \tau$, with ν_μ and ν_τ production occurring via neutral currents, and ν_e via both charged and neutral currents.

Since the neutronization occurs in the initial collapse, whereas the pair ν 's come from the 'thermally' radiating core, the timescale for the initial ν_e burst will be much less ($\lesssim 10^{-2}$) than the diffusion time (\sim seconds) that governs the emission of the bulk of the flux. Some so-called 'advection/convection' models increase the initial ν_e burst by convecting high- T , degenerate core material out. These models have higher-energy ν_e 's with larger fluxes, and suppress the $\bar{\nu}_e$ fluxes.

More than half of the neutrino emission comes out in the first second. The remaining comes out over the next few tens of seconds as the hot, newborn, neutron star cools down to become a standard 'cold' neutron star (c.f. 21). Detailed models such as Mayle et al.¹⁸ seem to find that the pair processes yield an appropriate equipartition of energy in the different species. The ν_μ and ν_τ 's have a higher energy / ν , thus their flux is down to preserve this equipartition.

Despite the explosive mechanism, for stars in the mass range $16 \lesssim M \lesssim 10M_\odot$ the most distinctive structure in the neutrino signal is the initial neutronization burst. However, in the delayed explosions seen by Wilson et al.⁹, for stars with $M \geq 16M_\odot$, besides the burst, the neutrino luminosity shows an oscillatory behavior superimposed on an exponentially decaying signal. The oscillations in luminosity are related to oscillations in the mass accretion rate onto the proto-neutron star. The physical nature of the instability that is responsible for the oscillations in luminosity and mass-accretion rate is described in Wilson et al.⁹, and in more detail in Mayle²². After the envelope is ejected, the luminosity will smoothly decrease as the remaining binding energy is emitted.

It is important to remember that the average neutrino luminosity, mean neutrino energy, and total emitted energy depend only on the initial iron-core mass and are otherwise independent of the explosive mechanism. Because the opacity is less for the ν_μ and ν_τ 's, they are emitted from deeper in the core where temperature is higher. Thus, they have a higher average energy. The calculations of Mayle et al.¹⁸ find $E_{\nu_\mu} \simeq E_{\nu_\tau} \approx 2E_{\nu_e}$. The

easier-to-observe $\bar{\nu}_e$ start out with energy comparable to ν_e 's and gradually shift over to the $\nu_\mu - \nu_\tau$ energy as their emission continues from progressively deeper in the core.

Each spectrum for neutrino species is reasonably well fit by a Fermi-Dirac (F-D) distribution with temperature T . However, in the detailed spectral analyzer that Mayle et al.¹⁸ carried out, it was found that the higher-energy neutrino fluxes were indeed higher than the single-temperature, F-D fit to the peak. Figures 1a-c showed the ν_e , $\bar{\nu}_e$, and ν_μ neutrino spectra for a $12M_\odot$ star with $\epsilon_B = 1.6 \times 10^{53}$ ergs. (Note that the ν_τ , $\bar{\nu}_\mu$, and $\bar{\nu}_\tau$ fluxes are identical to that of ν_μ .) (A $15M_\odot$ model gives essentially the same results but with a higher luminosity due to their estimating a slightly more massive neutron star being formed with the consequent greater binding energy realized.)

Also shown on Figure 1 is the cross-section weighted differential counting rate per kiloton H_2O detector, neglecting threshold effects. Notice that the $\bar{\nu}_e$ counting-rate curve peaks at ~ 20 MeV, well above the Kamioka (and Mt. Blanc) thresholds and comparable to the IMB threshold. The ν_μ counting-rate peaks at ~ 30 MeV, whereas the corresponding ν_e counting rate falls rapidly with E .

We'll wait until we analyze the individual detectors before discussing sensitivities to thresholds, etc. However, just by using simple, model-independent arguments, one obtains a crude $\bar{\nu}_e$ counting rate for an H_2O detector

$$n = \frac{(1 - f_n)\epsilon_B}{2N_\nu \langle E_\nu \rangle} \frac{\langle \sigma \rangle}{4\pi r^2} \frac{2}{18} \frac{M_D}{m_p}$$

where f_n is the fraction radiated in the neutronization burst, $\langle E_\nu \rangle$ is the average neutrino energy, $\langle \sigma \rangle$ is the average cross section above threshold (see Appendix: while the cross section is reasonably well known, many authors have been careless here), r is the distance to the LMC ≈ 50 Kpc, M_D is the mass of the detector, m_p is the proton mass, and N_ν is the number of neutrino flavors. (For the Mt. Blanc liquid-scintillator detector, one should multiply by 1.39 for the average number of free protons in $H_{2+2n}C_n$.) Using F-D statistics yields

$$\langle \sigma \rangle = \frac{\int_{E_c}^{\infty} \bar{\sigma} \frac{E^4 dE}{1 + e^{E/T}}}{\int_0^{\infty} \frac{E^2 dE}{1 + e^{E/T}}}$$

where E_c is the low-energy cut-off and $\bar{\sigma} \equiv \sigma/E_\nu^2$. Later, we'll discuss E_c and trigger efficiencies, however, for now let us do the crude estimate that everyone did before real data existed. (We won't bother to reference any post SN theoretical papers on predicted counts since the calculation was done in all the detector proposals other than for $1/r^2$ scaling.) Namely, let $E_c \rightarrow 0$, then

$$\langle \sigma \rangle \approx 7.5 \times 10^{-44} 12 T_{\bar{\nu}_e}^2 \text{ cm}^2 = 12 \bar{\sigma} T_{\bar{\nu}_e}^2$$

Prior to SN1987a, estimates were made for distances within our galaxy. With the LMC these had to be scaled by r^2 . For completeness, let us plug in the standard numbers, $\epsilon_B = 2 \times 10^{53}$ ergs, $N_\nu = 3$, $f_n = 0.1$, and $T_{\bar{\nu}_e} \sim 4$ MeV. Thus,

$$n = 5.2 \left(\frac{T}{4 \text{ MeV}} \right) \left(\frac{\epsilon_B}{2 \times 10^{53} \text{ ergs}} \right) \left(\frac{1 - f_n}{0.9} \right) \frac{1}{(N_\nu/3)} \left(\frac{M_D}{\text{ktons}} \right) \left(\frac{50 \text{ kpc}}{r} \right)^2$$

For the 2.14 kiloton Kamioka detector, this yields 11 counts. Similarly, for the Mt. Blanc detector with 0.09 kilotons, times 1.39 extra, free protons in the scintillator, a simple

prediction is ~ 0.6 counts. IMB is a little more difficult because its threshold is not below the peak $\bar{\nu}_e$ counting rate. In addition, it is totally dominated by the high T tail where a constant T may not be an ideal approximation. However, we can crudely estimate that $\sim 50\%$ of the $\bar{\nu}_e$ counting rate is above the approximate IMB low E cut-off of 20 MeV. Thus, with 5 kilotons, IMB should roughly get 13 effective counts. If we are more careful regarding efficiencies' thresholds and integrals over F-D distributions we reduce this prediction to 6. However, even the crude estimates show about what one naively expected from supernova theory independent of detailed models.

To estimate the expected number of electron scattering events, one can numerically integrate the differential counting rate curves derived from Mayle et al. with thresholds and find that for every 10 $\bar{\nu}_e$ absorptions, one expects about 0.7 ν_e scattering and about 0.7 $\nu_x e$ scattering, where ν_x is either ν_μ , $\bar{\nu}_\mu$, ν_τ , $\bar{\nu}_\tau$, or $\bar{\nu}_e$. We can understand why the scattering rate is $\sim 1/15$ even though the cross section ratio at 10 MeV is ~ 80 by remembering that there are five electrons for each free proton in an H_2O target. In addition, at a given energy from our cross section table

$$(\sigma_{\nu_e} + \sigma_{\nu_\mu} + \sigma_{\bar{\nu}_\mu} + \sigma_{\nu_\tau} + \sigma_{\bar{\nu}_\tau} + \sigma_{\bar{\nu}_e})/\sigma_{\nu_e} \simeq 1.$$

Thus, if fluxes are equal, the rate is doubled. Actually, average energy of other species is about twice that of ν_e , but fluxes are reduced accordingly to roughly maintain equipartition of energy per neutrino species, thus keeping scattering constant.

For the 615-ton C_2Cl_4 Homestake there are $2.2 \times 10^{30} Cl$ atoms. As seen from the Appendix, the cross section is not a simple integer power of E_ν , however, it seems to fall roughly between an E^3 and E^4 relationship for $E_\nu \lesssim 30$ MeV. For an E^3 dependence, the number of expected counts, n_3 , from a thermally-averaged distribution with temperature, T_{ν_e} ,

$$n_3 \simeq 0.15 \left(\frac{T_{\nu_e}}{\text{MeV}} \right)^2 f_{\nu_e} \left(\frac{\epsilon_B}{2 \times 10^{53} \text{ergs}} \right) \left(\frac{50 \text{kpc}}{r} \right)^2$$

and for an E^4 dependence

$$n_4 \simeq 0.06 \left(\frac{T_{\nu_e}}{\text{MeV}} \right)^3 f_{\nu_e} \left(\frac{\epsilon_B}{2 \times 10^{53} \text{ergs}} \right) \left(\frac{50 \text{kpc}}{r} \right)^2$$

where the fraction of ν_e 's is

$$f_{\nu_e} = f_n + \frac{1 - f_n}{2n_\nu} \approx 0.25$$

in the standard model with $T_{\nu_e} \simeq 3.5 \text{MeV}$, but approaches unity in some non-standard advection models with T_{ν_e} approaching 10 MeV.

Thus, for $T_{\nu_e} = 3.5 \text{MeV}$, $n_4 = 2.4 f_{\nu_e}$ and $n_3 = 1.8 f_{\nu_e}$, and for $T = 5 \text{MeV}$, $n_4 = 6.9 f_{\nu_e}$ and $n_3 = 3.8 f_{\nu_e}$. For temperatures above 5 MeV, the peak contribution to the thermal average would be coming from energies above 30 MeV where the cross section no longer rises as rapidly and the simple analysis above breaks down and the expected counting rate no longer continues to rise with temperature. A rough approximation for $T > 5 \text{MeV}$ might be

$$n \sim 5 f_{\nu_e} \left(\frac{\epsilon_B}{2 \times 10^{53} \text{ergs}} \right) \left(\frac{50 \text{kpc}}{r} \right)^2$$

In the standard case with $f_{\nu_e} = 0.25$ and $T = 3.5$, one expects about a half of a count above the background. However, for advection models, one might obtain several ^{37}Cl events. Similar to the solar case, ^{37}Cl is once again a potentially sensitive thermometer.

All the predictions described above assume a simple, spherical symmetric collapse. If large amounts of rotation or magnetic fields were present (with energies comparable to the binding energy) then the standard model would be altered with different time scales and different core masses and binding energies, since such conditions would alter the initial core mass as well as the dynamics. We will see that the Kamioka/IMB neutrino burst fits the standard assumptions well so that the collapse which created that burst did not have significant rotation or magnetic fields.

Before SN1987a, it was also obvious that a supernova, if detected by its neutrinos, would constrain neutrino properties. In particular, if the neutrinos got here, we'd have a lifetime limit. If the time pulse wasn't too spread out, that would mean a mass limit on those neutrino types that were clearly identified. Also, from the number of $\bar{\nu}_e$ counts, one could constrain N_ν since if N_ν was large, the fraction of thermally produced $\bar{\nu}_e$'s would go down. In addition, neutrino mixing could be constrained by detecting different types and comparing; with Mikheyev–Smirnov²³ matter mixing, as parameterized to solve the solar neutrino problem, $\nu_e \rightarrow \nu_\mu$ (or ν_τ), and ν_μ (or ν_τ) $\rightarrow \nu_e$, but nothing happens in the antineutrino sector. Such mixing would eliminate seeing the initial ν_e burst, but give higher energies to the later, thermal ν_e since they'd be mixed ν_μ 's (see Walker and Schramm²⁴). Of course, non-solar Mikheyev–Smirnov can be used if antineutrino mixing is seen. All of these effects will be examined with the data from SN1987a.

NEUTRINO OBSERVATIONS

Table 2 summarizes the neutrino observations, noting two reported neutrino bursts. Before discussing the plausibility of the first event, it is important to note that *all* neutrino detectors clearly had a detection on February 23rd near 7h 35m U.T. Thus, unquestionably *extra solar system neutrino astronomy has been born!* Let us now examine the burst Mt. Blanc reported on February 23rd, -2:52 with five events which was unsubstantiated by the other three detectors. While lack of concordance is easy to understand for IMB and Baksan, due to their higher thresholds, the lack of a strong concordant signal, significant above background, is difficult with regard to Kamioka. The Kamioka detector is 2140 tons, compared to 90 tons for Mt. Blanc, and the thresholds are similar. (Mt. Blanc was designed to detect $\bar{\nu}_e$'s from collapses in our galaxy, not the LMC.) Thus, many people have dismissed this first event as an unfortunate statistical accident. *A posteriori* statistics are difficult. While the chance of background exactly duplicating this event configuration eight hours before the visual outburst is low, perhaps the more relevant question is: What is the chance of background producing any plausible signal within two days prior to the visual detection? If any plausible signal is defined as three or more events (only three events were clearly above background) in less than or equal to 30 seconds, a chance occurrence becomes quite reasonable and many have assumed this explanation. However, one should be cautious in following popular opinion too rapidly. Detections near threshold can be tricky, and statistics of small numbers are notoriously suspect.

Kamioka did report that they had two background counts in the 10-minute interval centered at the Mt. Blanc event which is consistent with their background. However, de Rujula²⁵ has noted that if the IMB burst is used to accurately set the Kamioka U.T. clock

(which was only calibrated to $\sim \pm 1$ minute absolute), and the Kamioka background is scanned at precisely the U.T. of the first Mt. Blanc burst, then the two counts Kamioka sees over the 10-minute interval happen to fall within eight seconds of the Mt. Blanc event. While only one of these counts is clearly above threshold, this ‘chance’ occurrence has a probability of $1/80$ from the Kamioka background. Some have argued that the earlier Mt. Blanc burst time is easier to fit the light curve⁵. However, the 60-day continuously-rising light curve seems to require energy input from either a pulsar or radioactivity, so a simple pure shock-produced light curve does not yield a strong constraint. Table 3 shows the implied temperature and neutrino luminosity implied by the Mt. Blanc burst and the one or two Kamioka counts at that time. These were estimated by deconvoluting F–D distributions with thresholds and efficiencies. Notice that the burst reported at Mt. Blanc is not well fit by the standard collapse assumptions but instead requires lower-than-expected temperatures and extraordinarily high total energies.

Let us suspend our theoretical prejudice and ask if such a high-luminosity, low- T event did occur, would Kamioka have only seen one or two counts? In fact, as first noted by de Rujula²⁵ a minimal Kamioka detection cannot be totally excluded because the implied Mt. Blanc burst temperature is so low, and the thresholds are different. In particular, while playing with statistics of one or two events is clearly unreliable, it is worth noting that the two Kamioka events, if real, could also roughly imply conditions consistent with the Mt. Blanc burst, namely, low T and very high luminosities. The central values clearly differ. This argument has been quantified by de Rujula, to argue that there is a reasonable possibility that they could both be sampling the same distribution. The time structure of the Mt. Blanc event burst is also peculiar with one event four seconds before the rest. However, if both Kamioka events were real, it too would imply a long time structure, ~ 8 seconds. Some have also cited “ 3σ ” gravitational wave detector noise in Italy and Maryland in coincidence with the Mt. Blanc burst as significant. However, these are room temperature detectors with lots of noise and would imply $> 2000M_{\odot}$ emitted in gravitational waves. The Mt. Blanc burst would necessitate an initial collapse event that is quite different from standard models. Models with large magnetic fields and/or rotation, such as Symbalisy et al.²⁷ have low temperatures, but it is hard to imagine an event which radiates a *minimum* of an entire neutron star *rest mass* in neutrinos, or has a very non-thermal distribution. The non-standard event must then be followed by a subsequent collapse five hours later to a black hole or a dense, strange-matter star looking very much like a normal collapse, as we shall see. An alternative is that this event was not in the LMC but was *much* closer, thus reducing the energy requirements but requiring a remarkable timing coincidence. Given all these problems, this author is tempted to quote Eddington: “Observations should not be believed until confirmed by theory”. (However, if threshold effects are proven that lower Mt. Blanc’s and raise Kamioka’s so that the temperature increases and the luminosity drops, then theoretical models again become plausible.) Lack of firm theoretical support should not be interpreted as any fault on the part of the Mt. Blanc experimentalists who have done an impressive job and had the foresight to realize the potential importance of neutrinos from supernovae.

Let us now turn our attention to the well established Kamioka/IMB burst. (For a detailed discussion, the fact that Mt. Blanc and Baksan also have signals is irrelevant other than to show that detectors $\sim 1/20$ the mass can have $\sim 1/10$ the counts, due to statistics of small numbers plus possible background subtraction uncertainties.) Figure 2

is a plot showing the energy and timing of the Kamioka and IMB events. (Kamioka's event no. 6 is ignored as being below their criteria for a definitive event.) Note that almost all the counts concentrate in the first few seconds, as one expects in collapse models. The last events from IMB are the lowest energy ones of 20 and 24 MeV, which are the ones with the greatest uncertainty due to background subtraction. Figure 3 shows the number of counts/sec. If the two low-energy, late IMB counts are removed from IMB, note how well the two distributions track. It is easy to understand how IMB could have missed the late straggler Kamioka counts, since if real, they seem to be associated with low-energy events that are below the IMB threshold. A reasonable tail, as predicted by theory^{18,27}, would yield a counting rate after ten seconds $\lesssim 1/10$ times the integral of the peak (see Figure 8). Thus, one count is naively expected. Soviet calculations²⁸ yield a slower drop off with time and of course statistics on three are not that far from the prediction of one late count. Mayle and Wilson⁵² show that slight increases in neutron star binding energy, either from higher core mass (1.6 versus 1.4) or softer equations of state can lengthen the emission times significantly. A couple of counts after 10 sec is not a problem and even a 6-sec gap is not unreasonable with so few counts. In fact, the two late IMB counts would nicely fill in the gap.

To examine consistency let us use the number of counts and mean energies measured in the experiments to determine the implied temperature and energy emitted in $\bar{\nu}_e$'s. Such estimates require detailed consideration of efficiency and threshold effects. Figure 4 shows the efficiencies and thresholds reported for IMB and Kamiokanda. Note that thresholds are traditionally defined as efficiencies of 50%, thus experiments can get counts below threshold. For IMB, threshold is 29 MeV, for Kamiokanda, threshold is 8.5 MeV. In addition to the trigger efficiencies, there is also a low-energy cut-off where backgrounds become sufficiently high that confusion sets in. Kamioka assigned 20 photomultiplier (PMT) hits as a cut-off. This roughly corresponds to a cut-off energy, E_c , between 6 and 7.5 MeV. IMB discards events with less than 40 hits in their trigger-recording window. This roughly corresponds to a cut-off energy, E_c , between 18 and 21 MeV, in e^+ energies. While formally the Q value is 1.3 MeV, the actual difference between E_{e^+} and $E_{\bar{\nu}_e}$ depends on how the detectors are calibrated. At high energies both IMB and Kamioka use stopping muons, thus they don't include m_{e^+} , thus $Q_{eff} = 1.3$ MeV. At low energies, Kamioka calibrates with a γ source which might as a total calorimeter include m_{e^+} and m_{e^-} , thus, $Q = 2.3$ MeV, however, they use it so as to be mainly sensitive to compton electrons which again yields $Q = 1.3$. However, positrons are different from electrons in that they can annihilate in flight, thus yielding a different path distribution. As an approximation, $Q = 1.8$ MeV was used for Kamioka. However, calculations have been done for a range of assumed thresholds and Q -values to explore the sensitivity to the assumptions. From the efficiencies applied to the events, we can calculate weighted mean energies and the effective number of events. These are shown in Table 4 for various assumptions, such as assuming that the sub-threshold IMB events should be ignored, assuming the first two Kamioka events are electron scattering and should be ignored, assuming all Kamioka events below 10 MeV should be ignored, and assuming the final three Kamioka events should be ignored. Calculations were also done with and without correcting for the low-energy cross section deviation from E_ν^2 (see Appendix). Note that the use of higher cut-off energies eliminates lower energy, less confident events from dominating results due to their high weighting from their low efficiency.

To convert a mean neutrino energy to an effective temperature requires assuming that the emitted ν spectrum was well described by Fermi–Dirac statistics. Mayle et al. argue that this is a reasonable assumption, however, as mentioned before, they did find that their models had a higher tail at high energies than a simple, single-temperature model would yield. Thus, one might expect the IMB temperature to be slightly higher than the Kamioka temperature due to its weighting on the high-energy events. If the $\bar{\nu}$'s fit F–D statistics, then the mean energy ($\langle E_\nu \rangle$) as recorded by a detector with cross section proportional to E_ν^2 and cut-off energy E_0 , with efficiency of detection $f(E)$, is given below, where E and T are measured in the same units, and $E_0 = E_c(e^+) + Q$

$$\begin{aligned} \langle E_\nu \rangle &= \frac{\int_{E_0}^{\infty} \frac{f(E)E^5 dE}{1+e^{E/T}}}{\int_{E_0}^{\infty} \frac{f(E)E^4 dE}{1+e^{E/T}}} \\ &\simeq \frac{E_0 + 5T + 20\frac{T^2}{E_0} + \frac{60T^3}{E_0^2} + \frac{120T^4}{E_0^3} + \frac{120T^5}{E_0^4}}{1 + \frac{4T}{E_0} + \frac{12T^2}{E_0^2} + \frac{24T^3}{E_0^3} + \frac{24T^4}{E_0^4}} \end{aligned} \quad ()$$

which goes to the well known F–D integral values for $E_0 = 0$. Thus, we have a polynomial equation for T :

$$\begin{aligned} T^5 + \left(E_0 - \frac{\langle E_\nu \rangle}{5}\right) T^4 + \left(\frac{E_0^2}{2} - \frac{\langle E_\nu \rangle E_0}{5}\right) T^3 + \left(\frac{E_0^3}{6} - \frac{\langle E_\nu \rangle E_0^2}{10}\right) T^2 \\ + \left(\frac{E_0^4}{24} - \frac{\langle E_\nu \rangle E_0^3}{30}\right) T + \frac{E_0^5 - \langle E_\nu \rangle E_0^4}{120} = 0 \end{aligned} \quad ()$$

This latter equation can be trivially solved for the effective temperature, $T_{\bar{\nu}_e}(\langle E_\nu \rangle, E_0)$: from this equation it is obvious that the effective T is a very sensitive function of E_0 . Table 5 shows effective temperatures for the various assumptions with additional entries for variations in E_0 which leave numbers of events and mean energies unchanged. In Table 5, $\langle E_{\bar{\nu}_e} \rangle$ is $\langle E_{e^+} \rangle$ from Table 4 plus Q . In addition to using $\langle E \rangle$ to get T , we can use the effective number of counts to imply the amount of energy radiated in $\bar{\nu}_e$'s. Earlier, we saw that the observed number of e^+ counts, n in an H_2O detector is approximately related to the energy emitted in $\bar{\nu}_e$'s, $\epsilon_{\bar{\nu}_e}$, by the following relation

$$n \approx \frac{\epsilon_{\bar{\nu}_e}}{3.15T_{\bar{\nu}_e}} \frac{\langle \sigma \rangle}{4\pi r^2} \frac{2}{18} \frac{M_D}{m_p}$$

where $3.15T_{\bar{\nu}_e}$ is the average $\bar{\nu}_e$ energy in a F–D distribution, r is the distance to the supernova, M_D is the mass of the detector, m_p is the mass of a proton, and $\langle \sigma \rangle$ is the cross section above E_0 averaged over a F–D distribution with

$$\langle \sigma \rangle = \int_{E_0}^{\infty} \frac{\bar{\sigma} E^4 dE}{1 + e^{E/T}} / \int_0^{\infty} \frac{E^2 dE}{1 + e^{E/T}}$$

As for energies, we will use efficiency weighted values for n so as to avoid the treatment of the efficiency function in the integral. Evaluating $\langle \sigma \rangle$ yields

$$\langle \sigma \rangle \approx \frac{7.5 \times 10^{-44}}{2} T_{\bar{\nu}_e}^2 \left(\frac{E_0^4}{2T^4} + \frac{2E_0^3}{T^3} + 6\frac{E_0^2}{T^2} + 12\frac{E_0}{T} + 12 \right) e^{-E_0/T} \text{cm}^2$$

again, a function that is sensitive to E_0 . The expression for n can be inverted to solve for $\epsilon_{\bar{\nu}_e}$ and that is entered in Table 5. The total energy, ϵ_T (which can be compared to neutron star binding energy, ϵ_B) is related to $\epsilon_{\bar{\nu}_e}$ by

$$\epsilon_T \approx \frac{2N_\nu \epsilon_{\bar{\nu}_e}}{(1 - f_n)}$$

where N_ν is the number of neutrino flavors and f_n is the fraction of energy emitted in the initial neutronization burst. The numbers in Table 5 are calculated assuming $N_\nu = 3$ and $f_n = 0.1$, with Kamioka having $M_D = 2.14$ kilotons, and IMB having $M_D = 5$ kilotons. Figures 5 show the expected number of events versus $T_{\bar{\nu}_e}$ for various cut-off assumptions, and total energies ϵ_T (with $N_\nu = 3$, $f_n = 0.1$). Notice how changes of cut-off energy, E_c , within uncertainties, create significant variations in expected count rates. Figure 6 is a plot of $\epsilon_{\bar{\nu}_e}$ (and ϵ_T) versus effective $T_{\bar{\nu}_e}$ as derived from the data sets, as per the procedure of Table 4. The boundaries of the region come from one σ errors in counts as well as the range of reasonable assumptions one might make about cut-off energies and stated experimental errors in energy.

While one might expect (from Mayle et al.) IMB to measure a slightly higher T , it is interesting that there is nevertheless a region of overlap where both data sets yield the same $T_{\bar{\nu}_e}$ and $\epsilon_{\bar{\nu}_e}$. It is particularly satisfying that this region of overlap is exactly where one might have expected a standard gravitational collapse event to plot, namely, $\epsilon_T \sim 2 \times 10^{53}$ ergs, $T \sim 4.5$ MeV. Similar conclusions were reached by Sato and Suzuki³⁰ and Bahcall et al.⁴⁸ using a different treatment than has been applied here. Once T and ϵ_T are determined one can use the luminosity–temperature relationship to solve for the radius, R , of the neutrinosphere and obtain, in our case, a few tens of kilometers in reasonable agreement with the standard models. It might be noted from the figure and the table that when one examines the data in detail, it doesn't seem to make much difference whether the IMB data includes the two low points or not; the other uncertainties dominate. Similarly, it doesn't seem to matter, with regard to the Kamioka data, whether or not the first two or the last three events are included. However, the high E_c Kamioka data set with minimal weighting effects does seem to yield those parameters which are closer to overlap with IMB and closer to expected supernova parameters. It is worth noting that the above analysis is very crude, Kolb et al.⁴⁷ have pointed out that simple converting of E_e to $E_\nu - Q$, as was done here, is inaccurate, and the boundaries used in Figure 6 do not have a quantitative statistical meaning. Nonetheless, the results are suggestive and more detailed analyses seem to yield similar conclusions^{30,48}. In addition, one *should always* remember that statistics of small numbers are dangerous.

The angular distribution data on IMB are unfortunately biased, due to a failure of one of their four power supplies eliminating part of their array. The angular distribution for Kamioka is shown in Figure 7. It appears to show an isotropic distribution with a possible slight excess in the direction of LMC. From the isotropic rate background and the angular resolution, the number of excess directed events (note, Kamioka only explicitly claims two probable scatterings, but considering resolution, etc., we feel that our estimate is reasonable) is $\sim 3 \pm 1.8$. Since $\bar{\nu}_e + p$ would yield an isotropic distribution, the number of directed electron scattering events should be relatively small, as might be expected by the ratio of cross sections. Using the results of the Mayle et al.¹⁸ $12M_\odot$ model, one expects ~ 1.5 such events in reasonable agreement with the observations. One also expects that

$\sim 50\%$ of these scattering events are higher energy ν_μ , ν_τ , $\bar{\nu}_\mu$, $\bar{\nu}_\tau$, or $\bar{\nu}_e$ events. This also fits well since the highest energy Kamioka events have $\cos\theta > 0.7$. It is also intriguing that the first two events had $\cos\theta$ closest to unity. Remember that the initial 0.01 sec neutrino burst is expected to be ν_e 's with no $\bar{\nu}_e$'s. While two such scatterings might be excessive considering the cross section suppression (unless the ν_e flux is slightly enhanced by advection convection) statistics of two versus one are not worth arguing about and are not useful in confirming or denying one theory instead of another.

While discussing ν_e scattering, its worth noting that the ^{37}Cl experiment of Davis was operating at the time of The Supernova, and counting began shortly after the light was observed. This experiment is only sensitive to ν_e 's. After 45 days of counting, Davis sees one count, completely consistent with his normal counting rate³¹. As mentioned before, for a standard collapse one expects from the LMC event ~ 0.5 events in the Homestake Chlorine detector. However, if one interprets the Kamioka data as implying a large excess²⁹ of ν_e 's, then one might have expected several ^{37}Cl counts. The lack of observed Cl counts argues that the ν_e flux is not in disagreement with standard predictions of $\sim 2 \times 10^{52}$ ergs of neutronization ν_e 's, plus 3×10^{52} ergs of thermal ν_e 's, all at $E_\nu \sim 10$ MeV ($T_{\bar{\nu}_e} \sim 3.5\text{MeV}$). This constrains models^{49,50} with 'advection' producing excessively large high-energy ν_e fluxes and reducing the $\bar{\nu}_e$ fluxes. As mentioned earlier, such models can predict at most about 5 ^{37}Cl counts. While extreme models with $T_{\nu_e} \gtrsim 5\text{MeV}$ and $f_{\nu_e} \sim 1$ may be in difficulty, intermediate models with $T_{\nu_e} \lesssim 4\text{MeV}$ and/or $f_{\nu_e} \lesssim 0.5$ are still allowed.

Before leaving the neutrino data, it cannot be emphasized too strongly that statistics of small numbers are *dangerous* and one must be extraordinarily careful *not to overly interpret* all the bumps, wiggles, and time delays. Impatience in waiting for a collapse event in our galaxy with ~ 100 times the counting rate is unfortunately stimulating such detailed interpretations of the only data we have. Conclusions drawn in this way must be appropriately normalized.

CONSTRAINTS ON NEUTRINO PHYSICS

Independent of detailed collapse models, or even whether or not the Mt. Blanc burst is real, we can use the detection of neutrinos from SN 1987a in the Kamioka and IMB detectors to constrain neutrino properties.

Neutrino Lifetime

Obviously, if $\bar{\nu}_e$'s made it over 50 Kpc, they must have a lifetime τ such that

$$\gamma\tau > 1.6 \times 10^5 \text{yr}$$

where γ is the relativistic factor ($\gamma = E_\nu/m_\nu$). Of course, to have decay requires $m_\nu > 0$. Since γ for ν 's from the sun is $\sim 1/10$, γ 's from supernovae (assuming $m_{\nu_e} = m_{\bar{\nu}_e}$) this means that neutrino decay is not a solution to the solar neutrino problem unless one combines decay with special mixing assumptions³².

Neutrino Mass

Since the neutrino bursts were relatively narrow in timespread, despite the energies being spread out over a range of about a factor of two, it is obvious that there cannot be too significant of a neutrino rest mass. While the relationship between mass, timespread and energy is derived in freshman physics the world over, the key here is to decide which

counts to use to get the time and energy spread, and to estimate what the intrinsic spread was in the neutrino burst in the absence of finite masses. It is these assumptions that have yielded more neutrino mass preprints than neutrino events observed. (Thus, we will not bother to reference them.)

Before discussing what we can say in a model-independent manner, it is important to emphasize that all we get model-independently is an upper limit on the mass, since it is certainly possible that the timespread is just due to intrinsic emission time, and not any mass effects. Thus, all papers claiming finite masses rather than upper limits are intrinsically model-dependent. In addition, since most, if not all, of the counts are $\bar{\nu}_e$'s, it is only reasonable to measure neutrino-mass limits for $m_{\bar{\nu}_e} = m_{\nu_e}$, not for any other neutrino species unless assumptions about mixing are made. (Of course anything else, like a fine-tuned photino, that interacts in H_2O with a rate similar to $\bar{\nu}_e$, and is produced in supernovae, would also be limited.)

Let us now plug some values into the standard relation for the mass implied by two particle of energy, E_1 and E_2 , emitted at the same time, but arriving 50 Kpc away with a separation Δt .

$$m = 20\text{eV} \left(\frac{E_1}{10\text{MeV}} \right) \left[\frac{(\Delta t/10\text{sec}) (E_2/E_1)^2}{(r/50\text{Kpc}) (E_2/E_1)^2 - 1} \right]^{1/2}$$

Model-independently, the simplest thing to do is to assume that the entire 13 sec spread of Kamioka was due to this effect. (IMB, with its higher energies, isn't able to constrain things as well.) Let us also assume that E_2 is the maximum, 35.4 ± 8 MeV, and E_1 is the minimum, 7.5 ± 2 MeV. To derive the extreme limit, let us note that the distance to LMC is at most uncertain by 10%, yielding a minimum r of 45 Kpc. In this extreme case, we obtain

$$m_{\bar{\nu}_e} < 23\text{eV}$$

However, if mass is really causing the spread, then the high-energy events should be first and the low-energy events, last. Thus, the maximum mass that could conceivable fit the time-sequenced data is found by taking the difference in time between the 35.4 MeV event and the highest energy late event. This yields a Δt of ~ 9 sec for the 13 ± 2.6 MeV event. The maximum, m , is found by characterizing E_1 with the highest possible final event energy 15.6, and the highest E_2 of 43.1 obtaining

$$m_{\bar{\nu}_e} < 30\text{eV}.$$

Even here we've had to assume that the supernova didn't conspire to emit the high energies late and the low energies early, and a higher mass gave us the nine second gap. We can use the two second bunching of the first events to argue that such conspiring did not spread them out too much.

To further restrict the mass, one can argue that if there was a 30 eV mass, why are the first events all clustered within two seconds, even though the energies differ by the full range. If one only uses the two second burst, then $m_{\bar{\nu}_e} \lesssim 10$ eV. However, such arguments are invoking some supernova-model bias, since it is conceivable that the higher-energy events occurred late in the collapse burst. In fact, the Mayle et al. detailed calculation yields exactly that behavior with a one second timescale, and their more recent calculations show this rising energy effect continuing for several seconds³⁷. In our case, this would yield

initial events having lower energies with less spread, followed by the later 35 MeV emission. The finite mass enables some of the low energy events to lag by ~ 10 sec, relative to the end of the initial burst. The problem is, why didn't the initial 20 MeV event have more than a 0.5 second separation from the 17.9 MeV event, for example. One might now conspire a little and have some low-energy emission start even before the 20 MeV event was emitted. The emission-burst times would be spread out over ~ 10 sec, rather than two, with the high- E emission coming toward the end. We would consider a 10 sec burst time (model bias!), the limit of plausibility. This limits an $m_{\nu_e} \lesssim 30$ eV. While the 30 eV limit can also be surmounted with a conspiratorial model, one can put some plausibility limits on the conspiracy. However, once we admit that the supernova limit is greater than the Zurich experimental limit³⁴ of $m_{\nu_e} < 20$ eV, the whole game becomes irrelevant, except for the curiosity that by having the supernova take place in LMC, the values come out very close to terrestrial laboratory measurements. This same conclusion was reached by Kolb et al.⁴⁷ using more detailed statistical arguments.

Alternative games of assuming two or more neutrino types of different mass run into the problem of low cross section for detection of all but $\bar{\nu}_e$. In addition, if the three late Kamioka events were a different neutrino with $m \sim 20$ eV, compared to the earlier burst with $m_{\bar{\nu}_e} \ll 20$ eV, one also has trouble understanding why these late events don't show any strong directional character, since they would then be electron-scattering events for either a $\nu_\mu + \bar{\nu}_\mu$ or $\nu_\tau + \bar{\nu}_\tau$. While it would be wonderful to have $m_{\nu_\tau} \approx 20$ eV, to give us the hot dark matter of the universe, this supernova cannot be used to prove it (or disprove it).

If specific models are assumed, far tighter limits can obviously be obtained. For example, Abbott, de Rujula and Walker⁵¹ using a very reasonable diffusing neutrinosphere model obtain a 90% confidence limit of $\bar{\nu}_e < 7$ eV.

Number of Neutrino Flavors

A limit to the number of neutrino flavors (with $m_\nu \lesssim 10$ MeV), N_ν , can be derived³⁹ from observation of the supernova-produced $\bar{\nu}_e$'s. The argument is based on the fact that in an equipartition of emitted neutrino luminosities among all flavors, the more flavors, the smaller the yield per flavor. Since $\bar{\nu}_e$ is only one flavor, this means that a detection of $\bar{\nu}_e$'s tells you immediately that the dilution by flavor could not have reduced the luminosity of $\bar{\nu}_e$'s below detectability. We can do this in a couple of ways; for example, from our simple relation for the predicted number of $\bar{\nu}_e$ counts in an H_2O detector, compared with the number observed, N_{obs} , we can calculate N_ν .

$$N_\nu \leq 3 \left[\frac{5.2}{n_{obs}} \left(\frac{T}{4\text{MeV}} \right) \left(\frac{\epsilon_B}{2 \times 10^{53}\text{ergs}} \right) \left(\frac{1-fn}{0.9} \right) \left(\frac{M_D}{\text{kton}} \right) \left(\frac{50\text{kpc}}{R_{LMC}} \right)^2 \right]$$

Using n_{obs} weighted by the detector-efficiency yields for Kamioka 16.5 ± 5 events (14.3 ± 4.3 if two events are electron scatterings). Putting in the deviations in the cross section from E_ν^2 only strengthens the limits.

$$N_\nu \leq (2 \pm 0.6) \left[\left(\frac{T_{\bar{\nu}_e}}{4\text{MeV}} \right) \left(\frac{\epsilon_B}{2 \times 10^{53}\text{ergs}} \right) \left(\frac{1-fn}{0.9} \right) \left(\frac{50\text{kpc}}{r} \right)^2 \right]$$

(If two events are assumed to be electron scattering, the 2 goes to 2.3.) From the concordant temperature prejudice, we can estimate that T is good to better than 25%. Similarly, ϵ_B

for $1.4M_{\odot}$ neutron-star models doesn't go over 3×10^{53} , independent of equation of state (or for an extreme limit with $1.6M_{\odot}$, we will also use 4×10^{53} ergs.) Obviously, $1 - f_n$ can't exceed unity. Allowing 10% uncertainty in r and putting in our extreme values yields

$$N_{\nu} < 6.3(9.1)$$

We hesitate to use this method with IMB data because of the need to be more careful with thresholds in $\langle \sigma \rangle$. An alternative technique is to use our explicit results for $\epsilon_{\bar{\nu}_e}$, as implied by the experimental detections. Since $\epsilon_{\bar{\nu}_e}$ was derived using detailed integrations of cross sections with cut-off energies, we don't have the cross section averaging uncertainty, implicit in the previous technique. Noting that with equipartition of energies

$$\epsilon_{\bar{\nu}_e} = \frac{(1 - f_n)}{2N_{\nu}} \epsilon_B$$

we can solve for N_{ν}

$$N_{\nu} = \frac{(1 - f_n)\epsilon_B}{2\epsilon_{\bar{\nu}_e}}$$

Fitting to the center of the IMB–Kamioka consistent range, we find $\epsilon_{\bar{\nu}_e} = 3.5 \times 10^{52}$ ergs, for $\epsilon_B = 2 \times 10^{53}$ ergs, and $1 - f_n = 0.9$. This yields

$$N_{\nu} = 2.9$$

If we take the extreme low value for $\epsilon_{\bar{\nu}_e}$, $1 - f_n$ of 1, and again allow ϵ_B to be 3×10^{53} ergs (4×10^{53}), we find the limit,

$$N_{\nu} < 5.5(7.3),$$

quite compatible with our more simply derived limit, ignoring thresholds and adjusting Kamioka data. This number is not as restrictive as cosmological bounds^{39,40} but is comparable to current accelerator limits⁴¹.

This argument can be used to limit any other sort of particle that might be emitted by the supernova and dilute the $\bar{\nu}_e$ energy share. For example, Ellis and Olive³⁶ use this argument to constrain the axion coupling to be $\gtrsim 10^9$ GeV, comparable to current red-giant limits³⁵. Using the fact that axions can escape from the higher T central core even though neutrinos cannot, we (Mayle, et al.³⁷) can further restrict axion coupling, possibly enough to eliminate the invisible axion.

Neutrino Mixing

If neutrino mixing occurs between emission and detection, it can obviously alter things. If the mixing is simple vacuum oscillations and the mixing length is short compared to 50 Kpc, then the chief effect will be an increase in the average ν_e , and to a lesser extent $\bar{\nu}_e$, energy, due to the oscillations with the higher energy ν_{μ} 's and ν_{τ} 's. Since we only reliably detect $\bar{\nu}_e$'s, this energy enhancement would be difficult to resolve. While some supernova models may need such enhancements to understand the IMB counts, others such as Mayle et al. do not; thus, no definite statements on mixing can occur. (The possibility of the electron scattering events having high energy is also still in the noise.)

Let us now address the matter mixing such as Mikheyev and Smirnov, and Wolfenstein²³ (MSW) have proposed. Walker and Schramm²⁴ have applied this to stellar collapse

scenarios. If this is indeed the solution to the solar neutrino problem, then only $\nu_e \leftrightarrow \nu_\mu(\nu_\tau)$ mixing is possible, not $\bar{\nu}_e \rightarrow \bar{\nu}_\mu(\bar{\nu}_\tau)$. Thus, the solar neutrino solution would not enhance $\bar{\nu}_e$ fluxes. It would deplete the initial neutronization burst. Since ν_μ cross sections are down by $\sim 1/6$, the possibility of seeing a neutronization scattering is significantly reduced. Thus, if the possible scatterings are real, standard adiabatic MSW is not the solution to the solar neutrino problem.

If we drop the solar neutrino solution and go to general MSW mixing, then we can mix $\bar{\nu}_\mu(\bar{\nu}_\tau)$ into $\bar{\nu}_e$, which might enhance the energy slightly, but would otherwise do little. No effect would occur for the electron scattering ν_e 's. As in the case of vacuum oscillations, no definitive statement can be made.

SUMMARY

SN 1987A has proven that our understanding of the basic energetics of gravitational collapse was quite reasonable once we included neutral current effects. Given that we now know what a neutrino burst looks like, we should have confidence that if a collapse occurs anywhere in our galaxy, regardless of the visibility of the SN, we should observe it. From SN rates in other galaxies like ours, we expect a rate of a collapse every 20 years or so and the neutrino flux will be up by $1/r^2$.

ACKNOWLEDGEMENTS

I would like to acknowledge useful conversations with John Ellis; Josh Frieman, Bruce Fryxel, Wolfgang Hillebrand, Ron Mayle, Keith Olive, Bill Press, Richard Schaefer, Albert Stebbins, Leo Stodolsky, Jim Truran, Terry Walker, Joe Wampler, and Jim Wilson. I particularly appreciate discussions with Michael Turner on cross sections and on ^{37}Cl , and Alvaro de Rujula on Poisson statistics and the Mt. Blanc consistency. I would also like to thank the Max Planck Institut für Physik und Astrophysik for their kind hospitality, and the Alexander von Humboldt Foundation for its support. This work was supported in part by NSF at The University of Chicago and NASA at Fermilab.

APPENDIX I: Cross Sections

The cross section for $\bar{\nu}_e + p \rightarrow n + e^+$ can be written as

$$\sigma = \frac{G_F^2}{\pi} \cos^2 \theta_c (1 - \Delta_\mu + \Delta_\beta) \left(1 + \frac{3g_A^2}{g_V^2} \right) p_e E_e (1 + \delta)$$

where δ is the sum of the recoil, δ_{rec} , radiative, δ_{rad} , Coulomb, δ_C , and weak magnetism, δ_{wm} , corrections discussed by Vogel⁴²; G_F is the standard weak coupling; $\cos^2 \theta_c$ is the cabbibo angle; $\Delta_\mu - \Delta_\beta$ is the correction from muon- to beta-decay; g_A and g_V are the appropriate renormalized axial and vector currents; and $p_e E_e$ is the product of the positron energy times its momentum. The ratio g_A/g_V is directly measured with polarized beams⁴³ to be $-1.262 + 0.005$, which corresponds to a neutron halflife of 10.4 minutes when the Coulomb correction for neutron decay is taken into account⁴⁴. Using $\cos^2 \theta_c (1 - \Delta_\mu + \Delta_\beta) = 0.9689 \pm 0.0005$ and $G_F^2/\pi = 1.686 \times 10^{-44} \text{ cm}^2 \text{ MeV}^{-2}$ yields⁴⁶

$$\sigma = 9.426 \times 10^{-44} (1 + \delta) p_e E_e \text{ cm}^2$$

For the energies of interest the negative weak magnetism term dominates δ , but even it is generally small compared to the corrections induced by using E_ν^2 rather than $p_e E_e$.

$$\begin{aligned} p_e E_e &= E_e^2 \left(1 - \frac{m_e^2}{2p_e^2} \right) \approx E_\nu^2 \left(1 - \frac{Q}{E_\nu} - \frac{E_{rec}}{E_\nu} \right)^2 \left(1 - \frac{m_e^2}{2E_e^2} \right) \\ &\approx E_\nu^2 \left(1 - \frac{Q}{E_\nu} - \frac{E_\nu - Q + 1}{m_p} \right)^2 \end{aligned}$$

where Q is the difference between measured positron energy and E_ν . As mentioned in the text, Q depends on the method of detector energy calibration. The weak magnetism correction is only $\delta_{wm} \approx -0.0035 \frac{(E_\nu - Q)}{\text{MeV}}$. Figure A1 shows σ versus E_ν^2 for $Q = 1.3, 1.8$ and 2.3 MeV, with full δ corrections. At high energies both IMB and Kamioka have $Q = 1.3$ MeV; at lower energies Q is more problematic. Note that if the E_ν^2 dependence is used for convenience in F-D integrals, then the cross section peaks at

$$\frac{\sigma}{E_\nu^2} \equiv \bar{\sigma} = 7.5 \times 10^{-44} \text{ cm}^2$$

rather than the higher values that many authors use. Also note that for energies below ~ 15 MeV, $\bar{\sigma}$ is lower, which yields an effective lower efficiency in integrals, assuming E_ν^2 dependence.

Another cross section one must use carefully is $^{37}\text{Cl}(\bar{\nu}_e)^{37}\text{Ar}$. Bahcall⁴⁵ summarizes the situation with emphasis on the solar ν energy range, where the onset of the isobaric analogue state is critical and σ rises by almost E_ν^4 (see Figure A2). However, above 15 MeV this rise slows down to dependence more like $E_\nu^{2.7}$ or less as E_ν increases.

REFERENCES

1. K. Hirata, et al., *Phys. Rev. Lett.* **58**, 1490(1987).
2. R. Bionta, et al., *Phys. Rev. Lett.* **58**, 1494(1987).
3. M. Aglietta, et al., *Europhys. Lett.*, submitted(1987).
4. A. Pomansky, *Proc. XXIIInd Recontre de Moriond*, in press(1987).
5. W.D. Arnett, in *Explosive Nucleosynthesis* (University of Texas Press, Austin, 1973).
6. T. Weaver and S. Woosley, *Proc. Wilson Symposium*, ed. J. Centrella (1983).
7. H. Bethe and G. Browne, *Scientific American* **252**, 60(1985).
8. E. Baron, et al., *Phys. Rev. Lett.* **55**, 126(1985).
9. J. Wilson, et al., *Ann. N.Y. Acad. Sci.* **262**, 54(1975)
10. W.D. Arnett and D.N. Schramm, *Astrophys. J.Lett.* **184**, L47(1973); S. Woosley, et al., *Astrophys. J. Lett.*, submitted(1987).
11. S. Shapiro, in *Gravitational Radiation*, ed. L. Smarr (Oxford University Press, Oxford, 1978).
12. D. Kazanas and D.N. Schramm, *Nature* **262**, 671(1976).
13. D. Kazanas and D.N. Schramm, *Astrophys. J.* **214**, 819(1977).
14. D.Z. Freedman, D.N. Schramm and D. Tubbs, *Ann. Rev. Nucl. Sci.* **27**, 167(1977); and references therein.
15. T. Mazurek, *Astrophys. J. Lett.* **207**, L87(1976).
16. D. Schramm and W.D. Arnett, *Astrophys. J.* **198**, 629(1974).
17. J. Wilson, *Astrophys. J.* (1981).
18. R. Mayle, J. Wilson and D.N. Schramm, *Astrophys. J.*, in press(1987).
19. D.N. Schramm, J. Wilson and R. Mayle, in *Proc. 1st International Conference on Underground Physics*, in *Il Nuovo Cimento* **9C**, 443(1986).
20. D.N. Schramm, in *Proc. 2nd Dumann Symposium* p. 87(1976).
21. A. Burrows and J. Lattimer, "The Birth of Neutron Stars", preprint(1985).
22. R. Mayle, Ph.D. Thesis, University of California, Berkeley (available as Lawrence Livermore preprint UCRL 53713).
23. S.P. Mikheyev and A.Yu. Smirnov, *Il Nuovo Cimento* **9C**, 17(1986); L. Wolfenstein, *Phys. Rev.* **D17**, 2369(1978).
24. T. Walker and D.N. Schramm, *Phys. Lett.B*, submitted(1987).
25. A. de Rujula, CERN preprint TH4702(1987).
26. D. Tubbs and D.N. Schramm, *Astrophys. J.* **237**, 541(1975).
27. A. Burrows and J. Lattimer, *Astrophys. J.* **307**, 178(1985).
27. E. Symbalisky, et al., *Astrophys. J. Lett.* **291**, L11(1985).
28. Chechetkin, et al., in *Supernovae*, ed. D. Schramm (D. Reidel, Dordrecht, 1977).
29. J. Arafune and M. Fukigita, Kyoto preprint RIFP-693(1987).
30. K. Sato and H. Suzuki, Tokyo preprint UTAP-52(1987).
31. A. Burrows, in *Proc. Homestake Conference on Solar Neutrinos* (1984).
31. R. Davis, private communication.
32. J. Frieman and K. Freese, SLAC preprint(1987).
33. R. Mayle and J. Wilson, LLNL preprint(1987).
34. A. Kundig, *Proc. XXIIInd Recontre de Moriond*, in press(1987).
35. D. Dearborn, D. Schramm and G. Steigman, *Astrophys. J.* **302**, 35(1985).
36. J. Ellis and K. Olive, CERN preprint UMN-TH-605/87(1987).
37. R. Mayle, J. Wilson, J. Ellis, K. Olive, D. Schramm and G. Steigman, in prepara-

- tion(1987).
38. W. Brunish and J. Truran, *Astrophys. J.*(1983).
 39. D.N. Schramm, in *Proc. XXIIInd Recontre de Moriond*, in press(1987).
 40. G. Steigman, M. Turner, D. Schramm and K. Olive, *Phys. Lett.* **176B**(1986).
 41. D. Cline, et al., *Comments on Nucl. Part. Phys.*, in press(1987).
 42. P. Vogel, *Phys. Rev.* **D29**, 1918(1984).
 43. P. Bopp, et al., *Phys. Rev. Lett.* **36**, 919(1986).
 44. D. Wilkinson, *Nucl. Phys.* **A377**, 474(1982).
 45. J. Bahcall, *Rev. Mod. Phys.* **50**, 880(1978).
 46. I.S. Towner and J. Hardy, in *Atomic Masses and Fundamental Constants*, ed. O. Klepper (Darmstadt, 1984).
 47. E.W. Kolb, A. Stebbins and M.S. Turner, *Phys. Rev. D*, in press(1987).
 48. J. Bahcall, T. Piran, W. Press and D. Spergel, IAS preprint(1987).
 49. A. Burrows, University of Arizona preprint(1987).
 50. W.D. Arnett, University of Chicago preprint(1987).
 51. L. Abbott, A. de Rujula and T.P. Walker, Boston University preprint(1987).
 52. R. Mayle and J. Wilson, Livermore preprint(1987).
 53. S. Woosley, University of California, Santa Cruz preprint(1987).

FIGURE CAPTIONS

- Figure 1: The differential neutrino flux and counting rate versus energy from the Mayle, Wilson and Schramm $12M_{\odot}$ model. The counting rate neglects threshold effects.
- Figure 2: The energy and timing of the IMB/Kamioka events.
- Figure 3: The ν counting rates for IMB/Kamioka.
- Figure 4: The efficiencies for the 5,000-ton IMB and the full 2,140-ton Kamioka detector. Kamioka efficiencies for the 780-ton fiducial volume are slightly higher. (These efficiencies are from private communications with the experimental groups.)
- Figure 5: Counting rates versus neutrino temperature assuming a Fermi–Dirac distribution characterized by a single temperature, curves assume different total energies emitted and different thresholds.
- Figure 6: Emitted energy, $\epsilon_{\bar{\nu}_e}$ in $\bar{\nu}_e$ and total emitted energy, ϵ_T (assuming $N_{\nu} = 3$) versus temperature for Kamioka and IMB data, allowing for statistical errors as well as systematic shifts due to possible electron scattering events and variations in threshold and efficiency assumptions. Note overlap region is a good fit to the standard model.
- Figure 7: Angular distribution of Kamioka data. If level of isotropic events is chosen from directions away from LMC, then there appears to be $\sim 3 \pm 1.8$ excess counts in the direction of the LMC, presumably due to electron scattering. The standard model predicts ~ 1.5 .
- Figure 8: Total integrated energy emitted in neutrinos versus time for different equations of state and neutron star masses from the calculations of Mayle and Wilson⁵². Note that for soft equations of state the energy is still rising after ~ 10 sec. Thus, significant emission is still occurring. There appears to be no need to invoke new physics to get the ν burst to have a finite tail at ~ 10 sec, merely have a soft E.O.S. and/or a neutron star mass slightly above $1.4M_{\odot}$.
- Figure A1: The cross section, σ , for $\bar{\nu}_e + p \rightarrow n + e^+$ divided by E_{ν}^2 versus energy for different values of $Q \equiv E_{\bar{\nu}_e} - E_{e^+}$. The cross section includes corrections for weak magnetism, Coulomb, recoil and radiative effects, as well as phase-space factors. Note that for $E_{\nu} \lesssim 15$ MeV, $\bar{\sigma} \equiv \sigma/E_{\nu}^2$ decreases rapidly as the energy drops. For high energies, $Q = 1.3$ MeV is a reasonable fit to the energy calibration of the detectors.
- Figure A2: The $^{37}\text{Cl} (\bar{\nu}_e e) ^{37}\text{Ar}$ cross section divided by $E_{\nu_e}^3$ versus energy from the tabulation of Bahcall⁴⁵.

FIGURE 1a

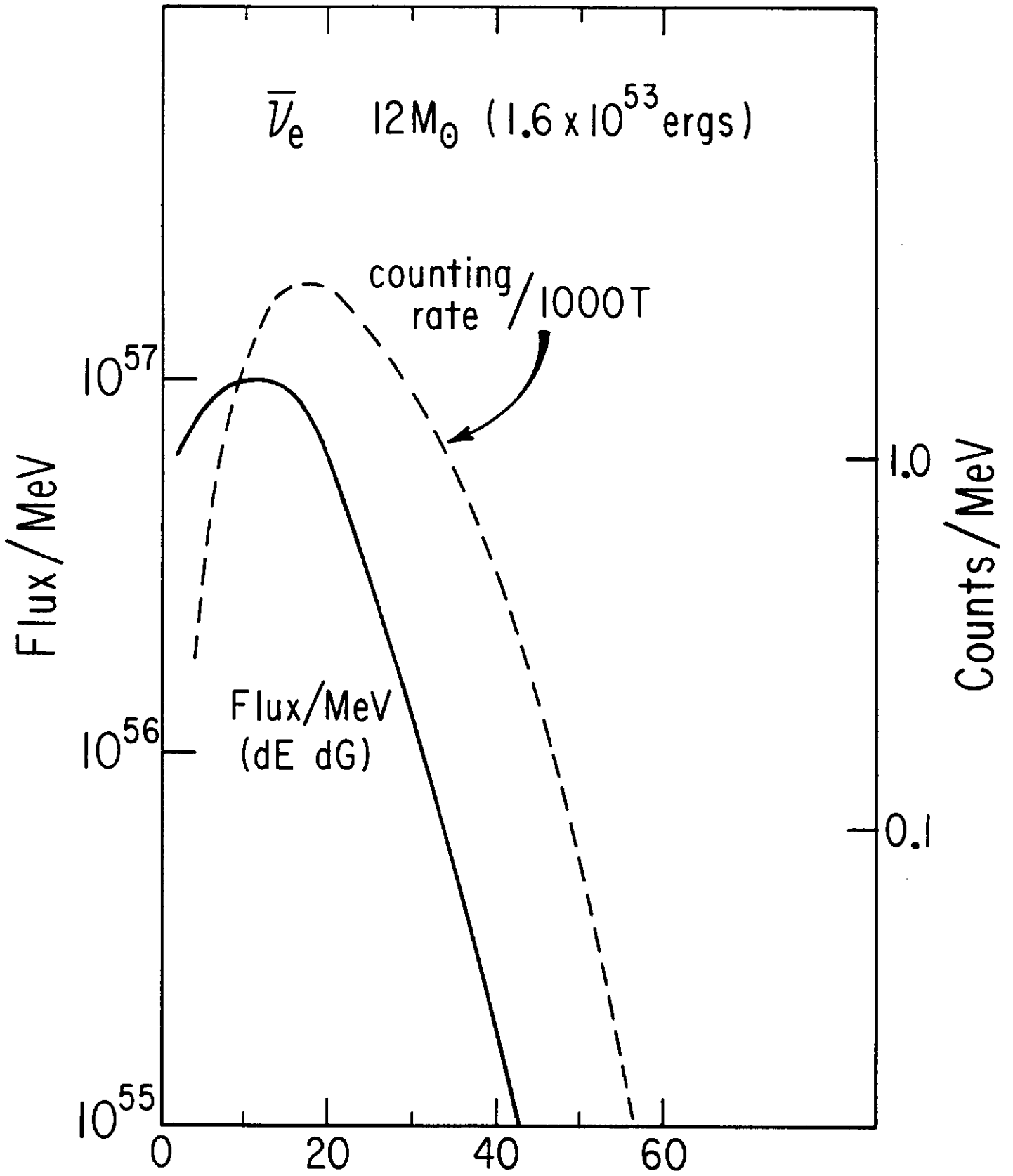


FIGURE 16

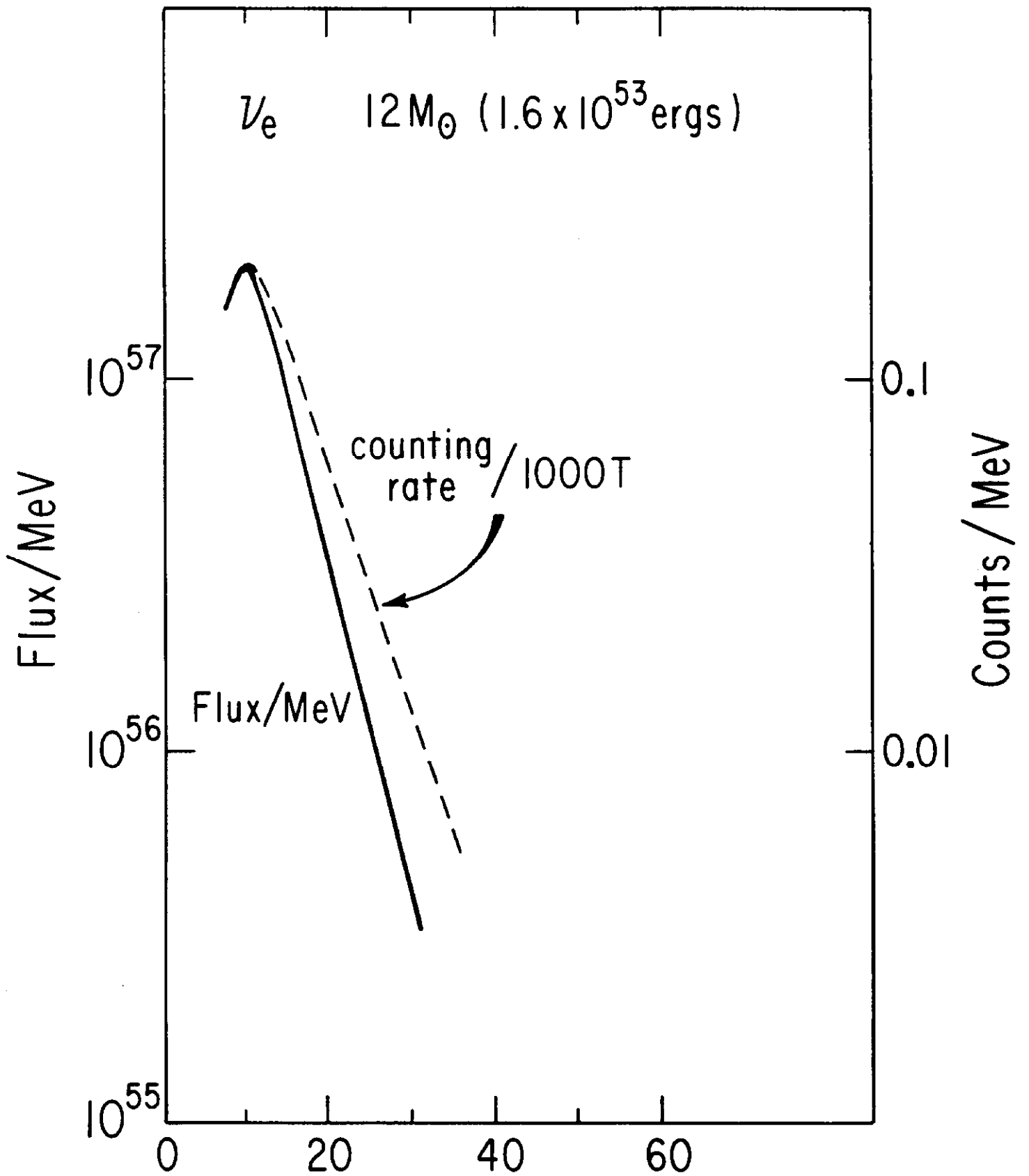
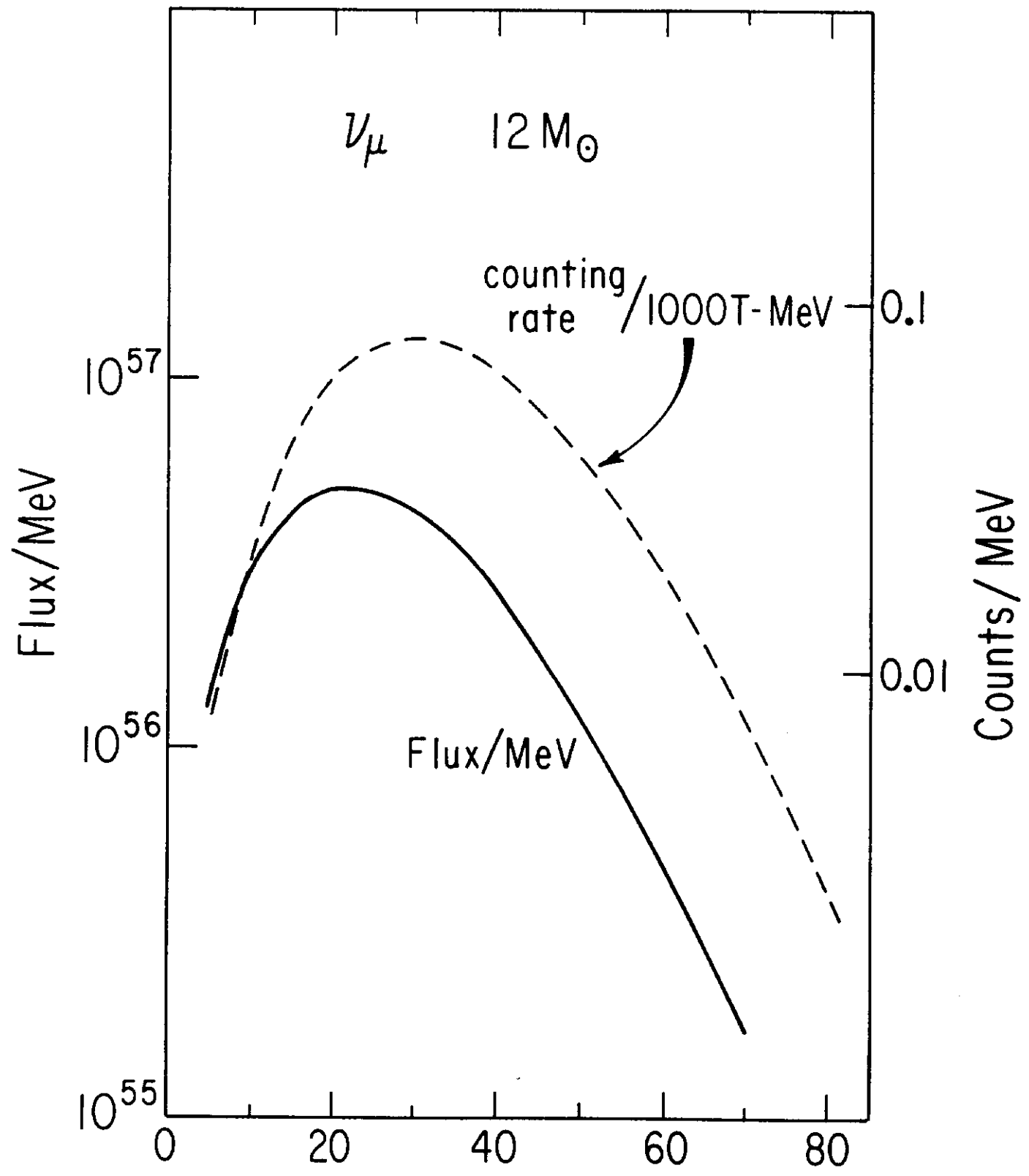


FIGURE 1c



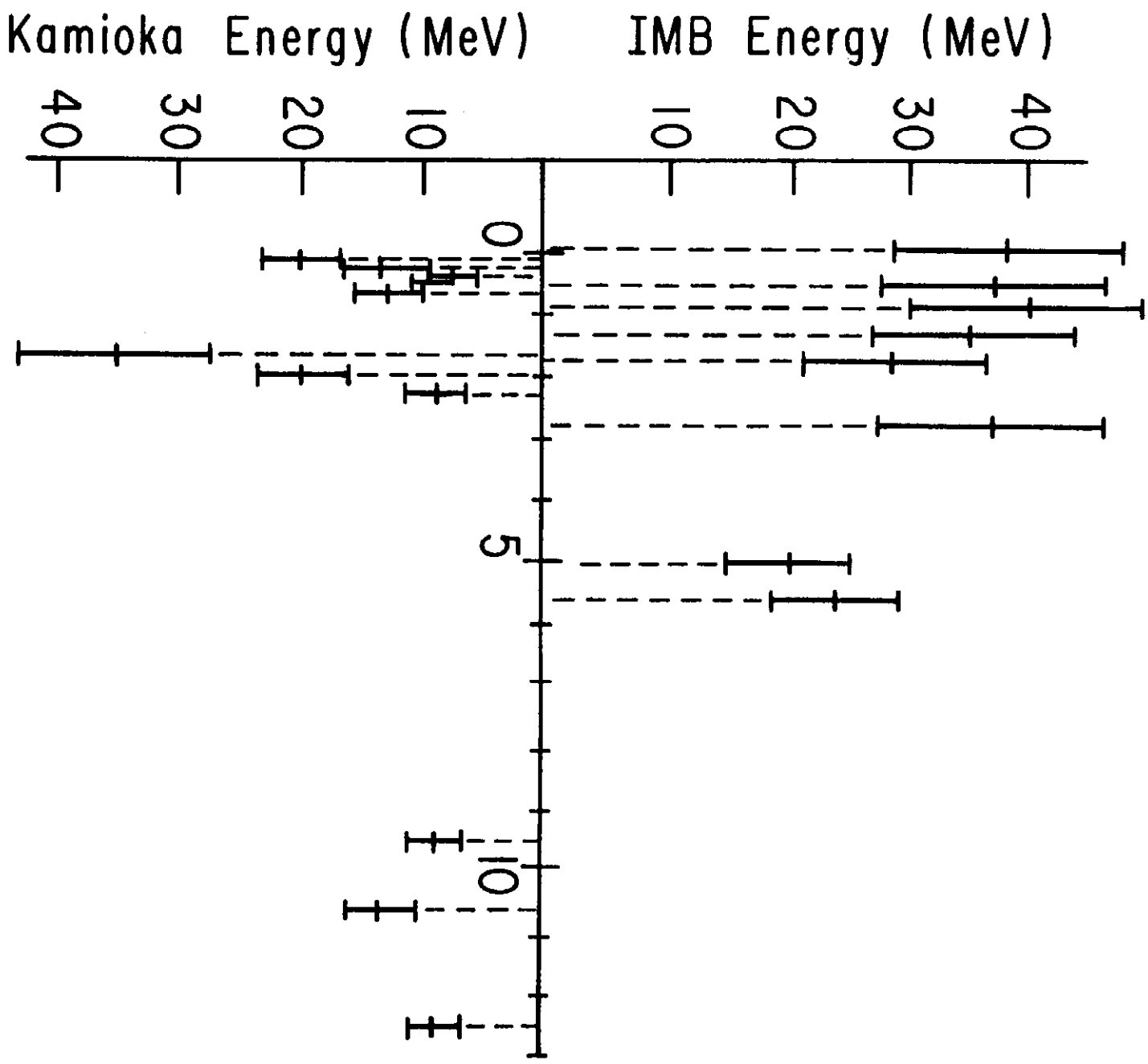


FIGURE 2

FIGURE 3

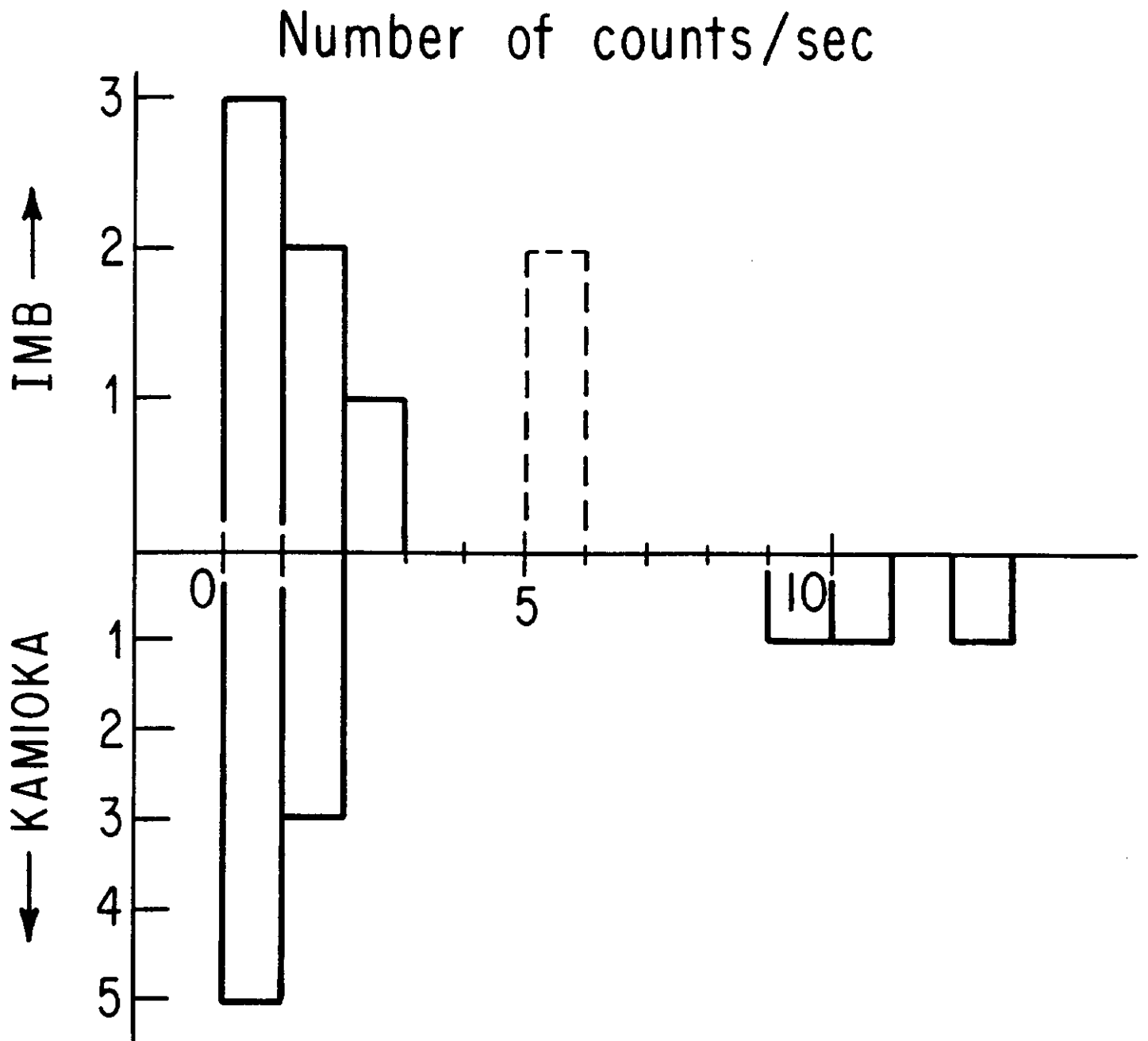


FIGURE 4

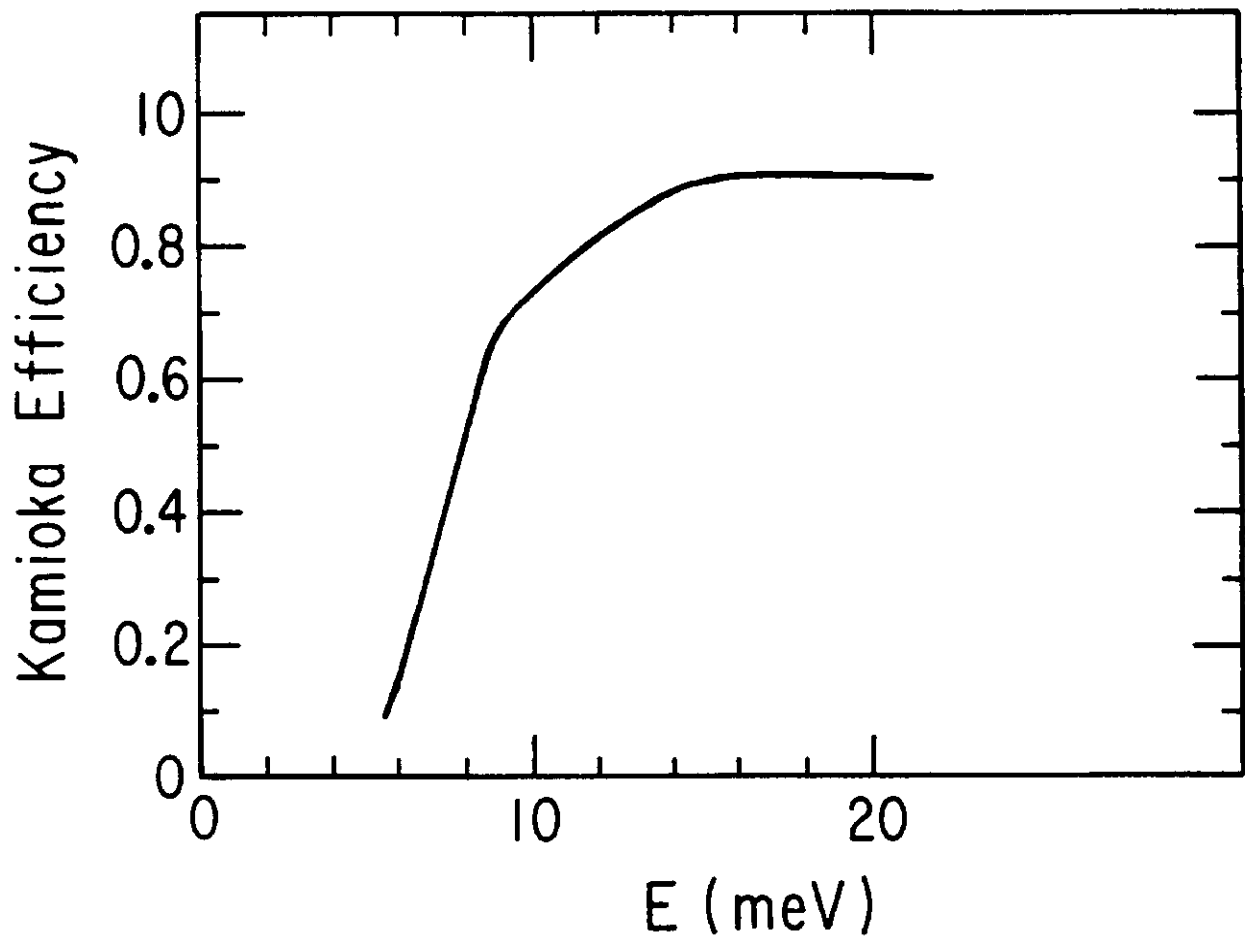
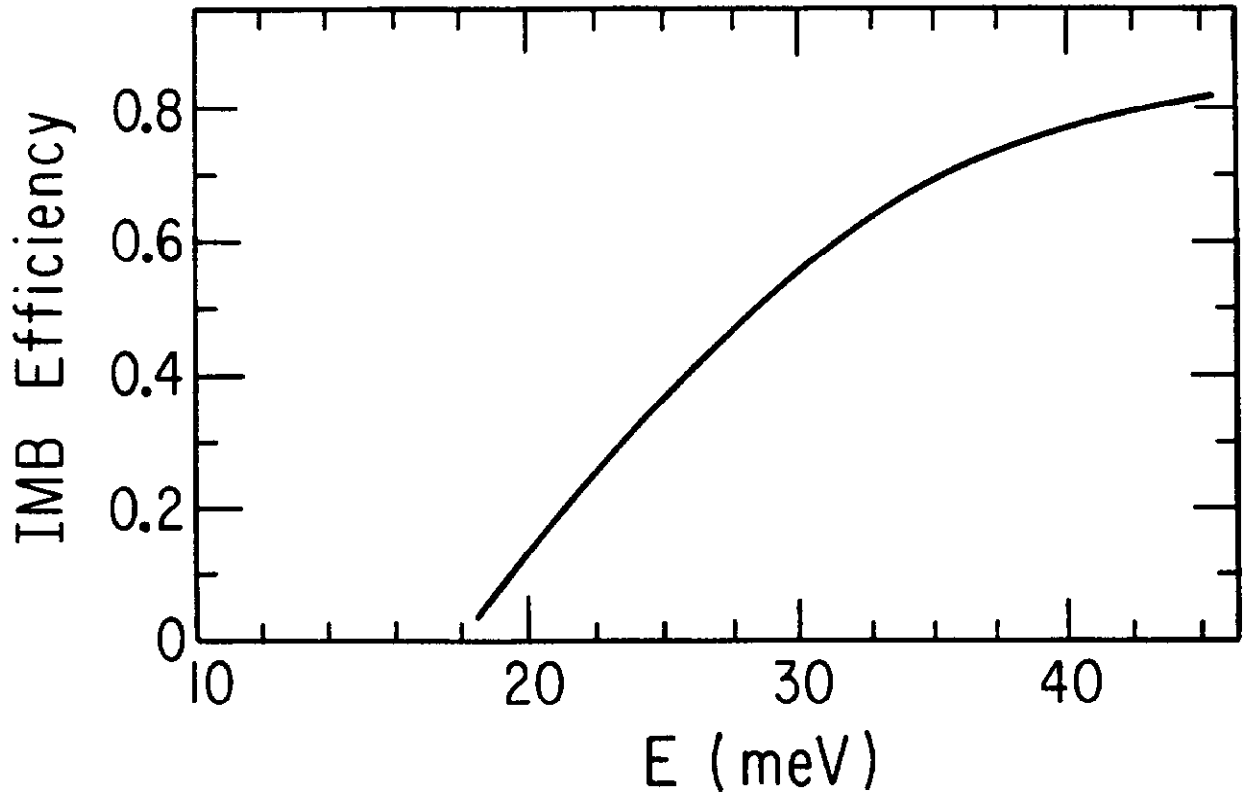
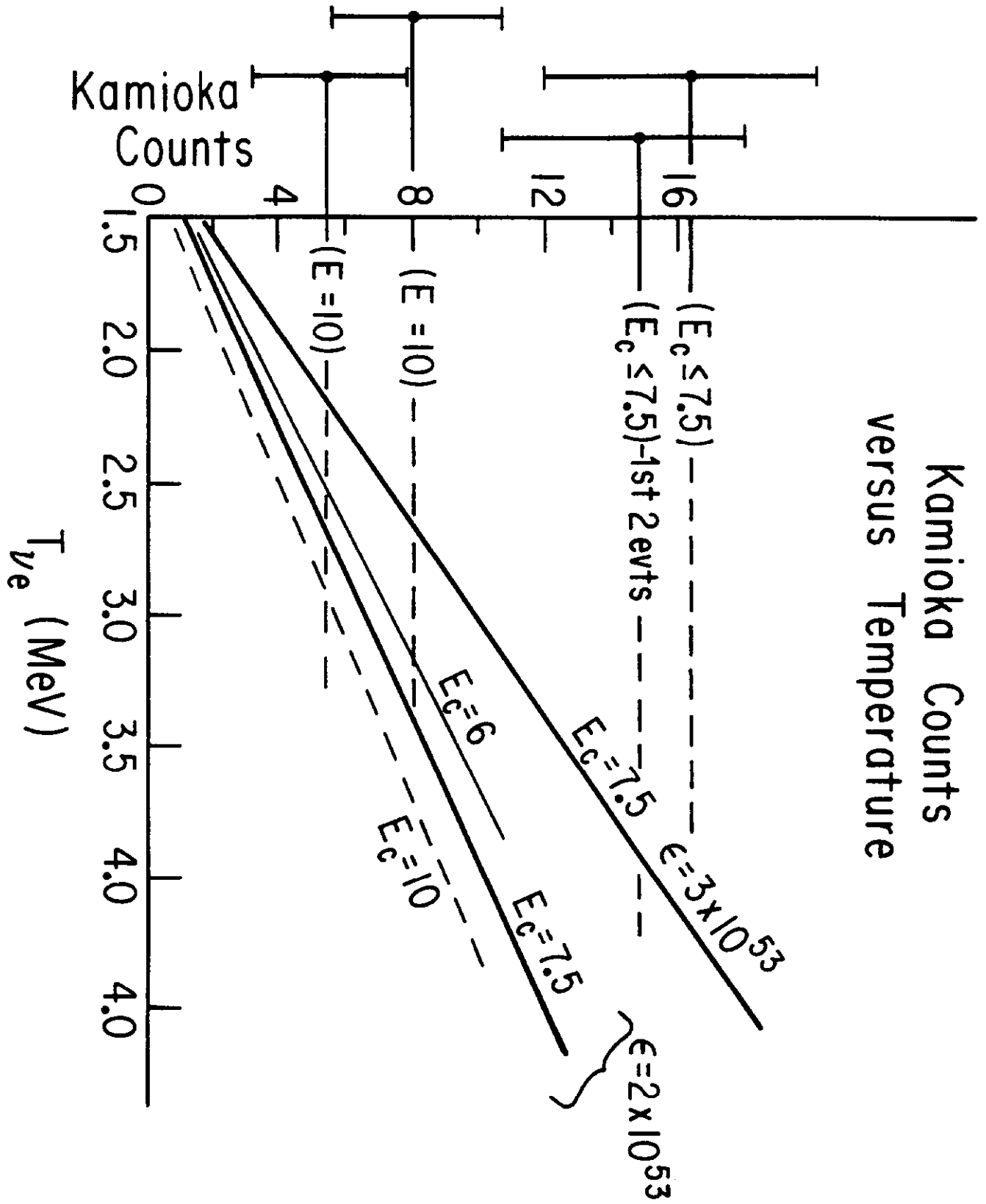


FIGURE 5a



IMB Counts
versus Temperature

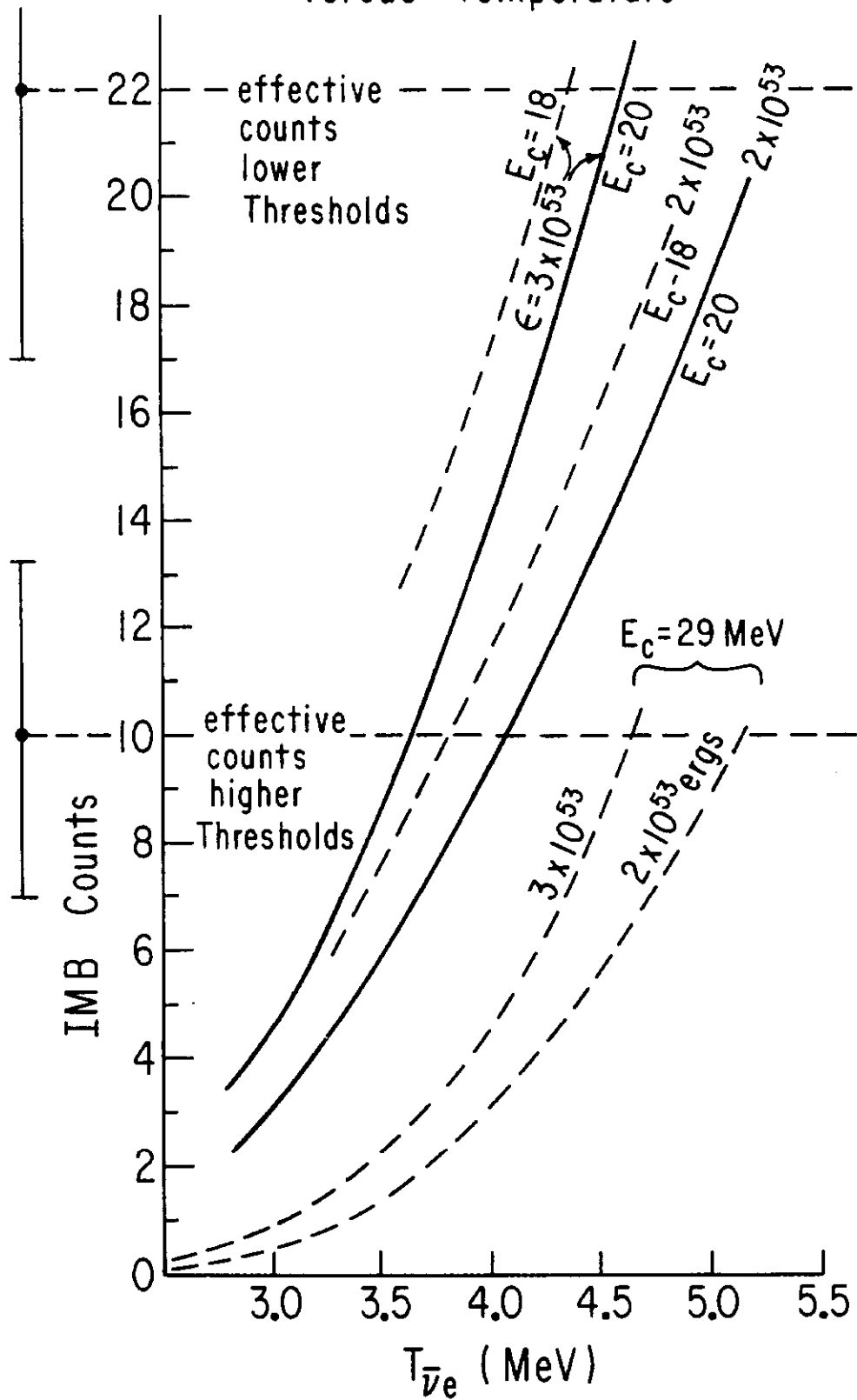
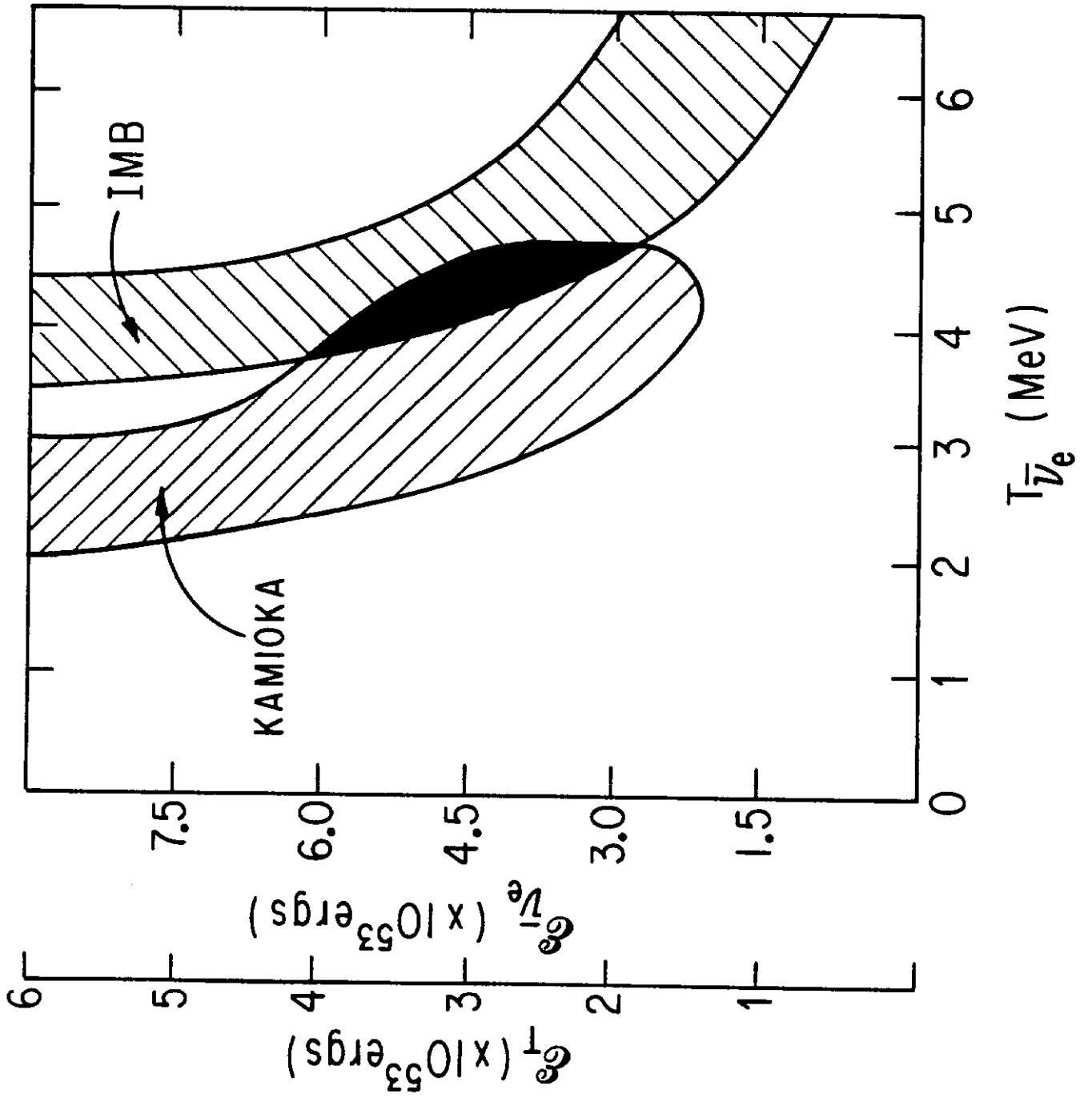


FIGURE 6



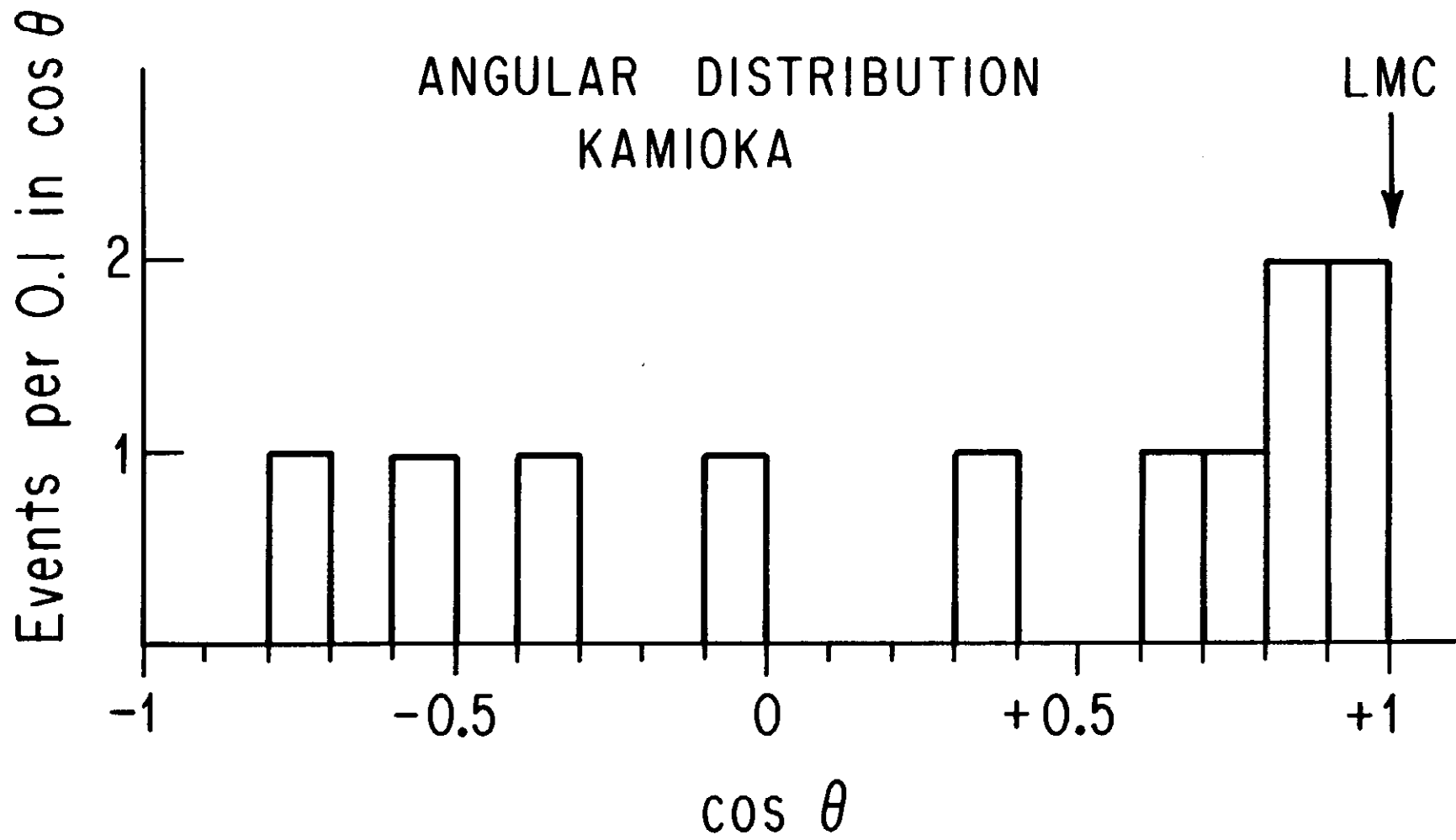


FIGURE 7

FIGURE 8

Energy Emitted vs Time

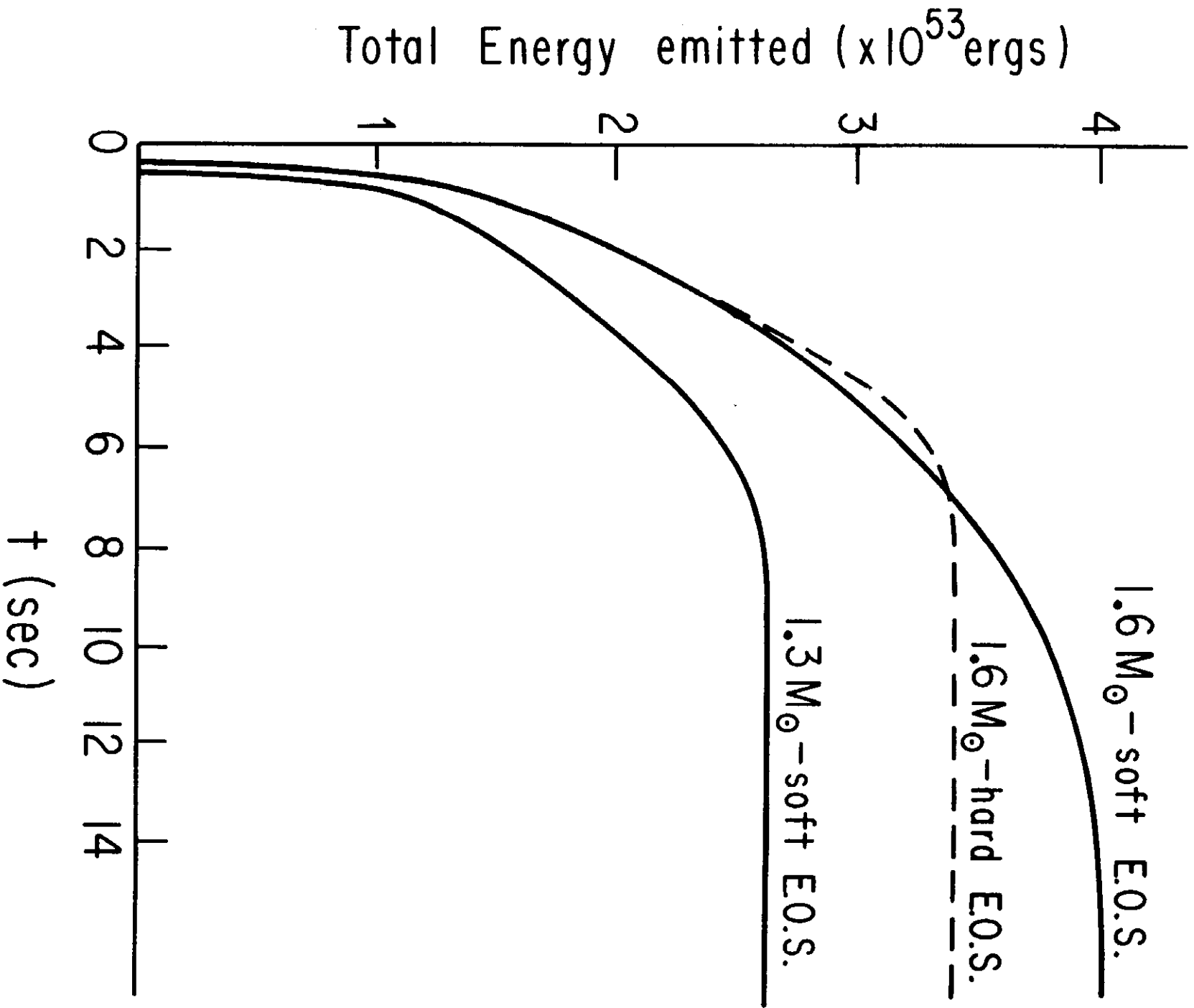


FIGURE A1

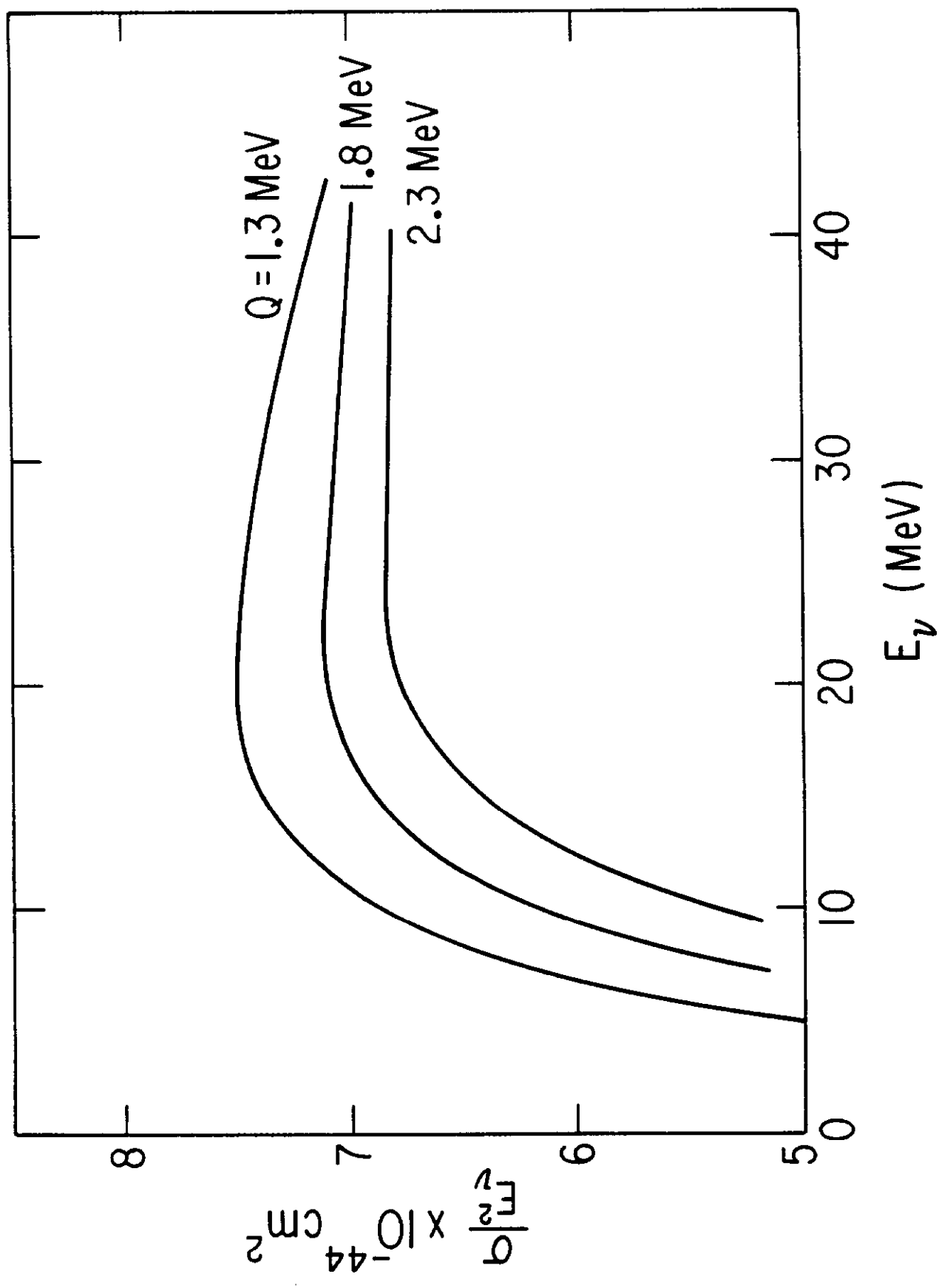
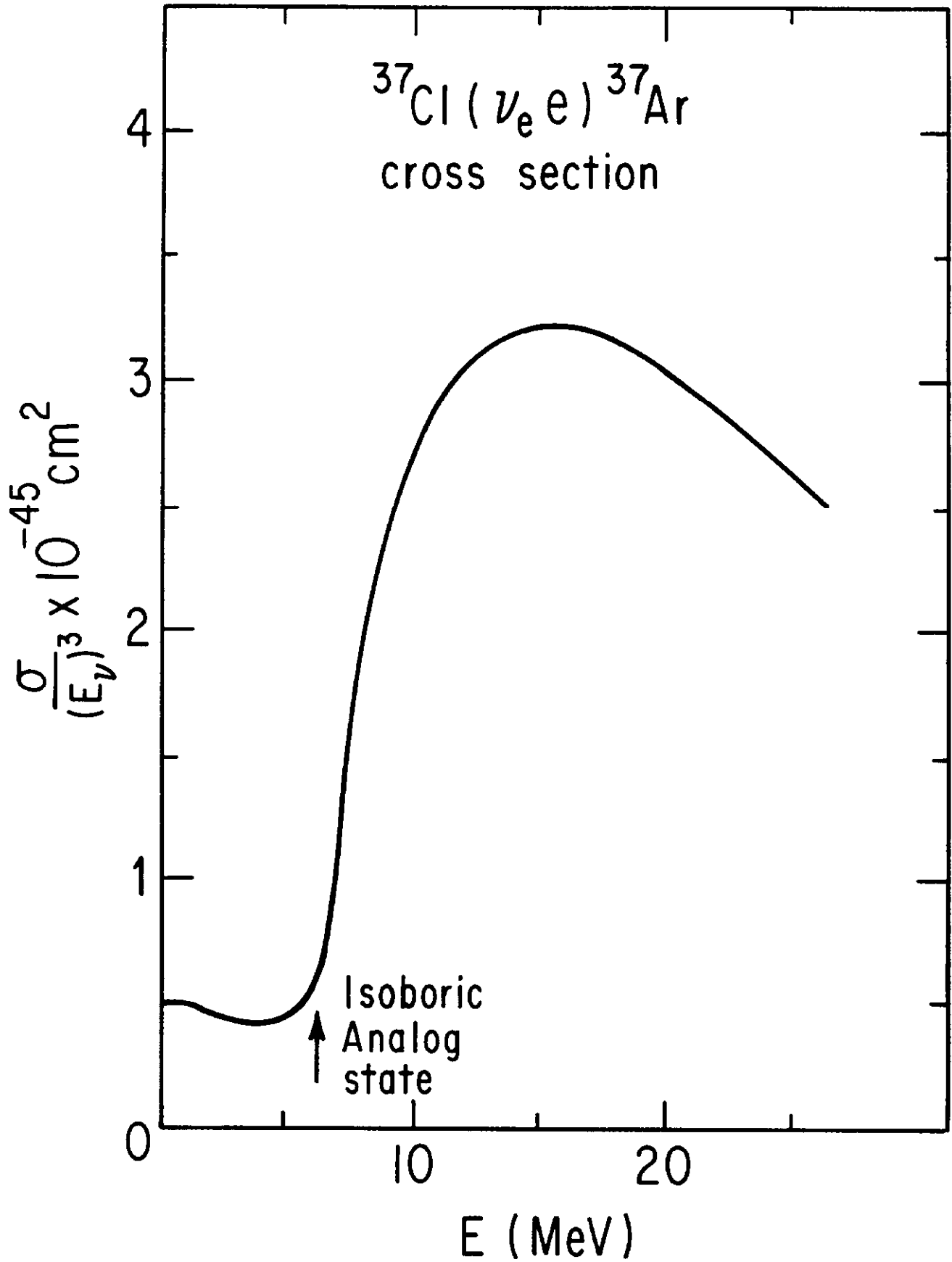


FIGURE A2



Interaction	$f(\xi)^*$	σ
$\nu_e e \rightarrow \nu_e e$	$(1/2 + \xi)^2 + (1/3)\xi^2 \approx 0.55$	$9.3 \times 10^{-45} (E_\nu/\text{MeV})\text{cm}^2$
$\bar{\nu}_e \rightarrow \bar{\nu}_e$	$(1/3)(1/2 + \xi)^2 + \xi^2 \approx 0.23$	$3.9 \times 10^{-45} (E_\nu/\text{MeV})\text{cm}^2$
$\nu_\mu e \rightarrow \nu_\mu e$	$(-1/2 + \xi)^2 + (1/3)\xi^2 \approx 0.09$	$1.5 \times 10^{-45} (E_\nu/\text{MeV})\text{cm}^2$
$\bar{\nu}_\mu e \rightarrow \bar{\nu}_\mu e$	$(1/3)(-1/2 + \xi)^2 + \xi^2 \approx 0.077$	$1.3 \times 10^{-45} (E_\nu/\text{MeV})\text{cm}^2$
$\nu_\tau e \rightarrow \nu_\tau e$	$(-1/2 + \xi)^2 + (1/3)\xi^2 \approx 0.09$	$1.5 \times 10^{-45} (E_\nu/\text{MeV})\text{cm}^2$
$\bar{\nu}_\tau e \rightarrow \bar{\nu}_\tau e$	$(1/3)(-1/2 + \xi)^2 + \xi^2 \approx 0.077$	$1.3 \times 10^{-45} (E_\nu/\text{MeV})\text{cm}^2$
$\bar{\nu}_e p \rightarrow n e^+$	see Appendix ($\sigma \propto p_e E_e$)	$(15 \lesssim E \lesssim 50 \text{ MeV})$ $7.5 \times 10^{-44} (E_\nu/\text{MeV})^2 \text{cm}^2$
$\nu_e^{16}\text{O} \rightarrow^{16}\text{Fe}^-$	see Arafune and Fukugita ²⁹	$1 \times 10^{-44} (E - 13 \text{ MeV})^2 / \text{MeVcm}^2$
$\nu_e^{37}\text{Cl} \rightarrow^{37}\text{Ar}^-$	see Appendix	$8 < E < 15$ $4.6 \times 10^{-46} (E_\nu/\text{MeV})^{3.7} \text{cm}^2$ $15 \lesssim E \lesssim 30$ $1.1 \times 10^{-41} (E_\nu/15 \text{ MeV})^{2.7}$

*Electron Scattering

$$\sigma = \sigma_0 f(\xi)s$$

$$\sigma_0 = \frac{G_F^2}{\pi} (\hbar c)^2 = 1.69 \times 10^{-44} \text{cm}^2 \text{MeV}^{-2}$$

$$\xi = \sin^2 \theta_w \approx 0.23$$

$$\text{For neutrino-electron interactions: } s \approx (2 \text{ MeV})(E_\nu \approx 1.02 \left(\frac{E_\nu}{\text{MeV}}\right) \text{ MeV}^2$$

(Note: In stars, degeneracy factors, kinematic transformations and thermal averages must be taken into account; see Tubbs and Schramm²⁶.)

Time (UT) February	Detector (threshold*/size)	# of Events (E-range/Duration)
23 2h 52m	Mt. Blanc (7 MeV/90 T) ⁺	5 (6-10 MeV/7 sec)
" ± 1 min	Kamioka (8 MeV/2.14 kT)	2 (7-12 MeV/10 sec)
"	IMB (30 MeV/5 kT)	none reported
"	Baksan (11 MeV/130 T) ⁺	none reported
23 7h 35m (± min)	Kamioka (7 MeV/90 T)	11 (7-35 MeV/13 sec)
23 7h 35m	IMB (30 MeV/5 kT)	8 (20-40 MeV/4 sec)
"	Baksan (11 MeV/130 T) ⁺	3 (12-17 MeV/10 sec)
"	Mt. Blanc (7 MeV/90 T) ⁺	2 (7-9 MeV/13 sec)
sum of pulses	Homestake ν_e (0.7 MeV/615 T) ^{**}	consistent with background
Optical		
23 9h 25m	lack of sighting	$m_\nu \gtrsim 8$ magnitude
23 10h 40m	photograph	$m_\nu = 6$ magnitude
24 10h 53m	discovery	$m_\nu = 4.8$ magnitude

*Threshold is when efficiency drops to $\leq 50\%$ (sub-threshold events are therefore possible).

⁺These detectors are liquid scintalators with $H_{2n+n}C_n$, thus have ~ 1.39 more free protons than H_2O detectors of same mass.

^{**}The Homestake detector is only sensitive to ν_e 's. It is made of C_2Cl_4 .

Table 3: The Mount Blanc Burst							
Mount Blanc Data							
	Mean E (MeV)	$\langle\sigma\rangle$	eff. T_{ν_e} (MeV)	$\epsilon_{\nu_e} (\times 10^{52} \text{ergs})$	$\epsilon_{total} (10^{53} \text{ergs})$		
all 5 events							
with 5 MeV cut-off	8.4	10.2	1.6	96 ± 42	64 ± 29		
with 7 MeV cut-off	8.4	10.2	0.3	$8 \pm 3 \times 10^{11}$	$5 \pm 2 \times 10^{11}$		
3 high events							
with 7 MeV cut-off	9.3	11.1	0.9	$3.6 \pm 1.6 \times 10^3$	$2.4 \pm 1 \times 10^3$		
with 5 MeV cut-off	9.3	11.1	1.8	44 ± 19	30 ± 13		
Kamioka (at the same time)							
	Mean E_{e^+}	Wt. Mean	e^+ eff. counts	$\langle E_{\nu_e} \rangle$	eff. T	$\epsilon_{\nu_e} (10^{52})$	$\epsilon_T (10^{53})$
Both events w/ 7.5 MeV cut-off	9.8	8.8	4.3	10.6	0.9	225 ± 160	150 ± 100
high event only w/7.5 MeV cut-off	12	12	1	13.8	2.0	1 ± 1	0.7 ± 0.7

Table 4: Events and Mean Energies for e^+				
	Number of Events	Unweighted Mean e^+ Energy (MeV)	Effective Number of Events	Weighted Mean e^+ Energy (MeV)
Kamioka				
$E_c = 6$	11	15.4	16.5	13.6
$E_c = 10$	7	19.4	7.8	19.3
$E_c = 6^*$	9	15.1	14.3	13.0
$E_c = 6^{**}$	8	17.4	11.6	15.2
$E_c = 6^\dagger$	5	20.4	5.6	20.3
$E_c = 6^\ddagger$	11	15.4	20.5	12.6
IMB				
$E_c = 18$	8	32.5	$19.4 \rightarrow 22^\ddagger$	27.9
$E_c = 29$	6	36	$9.1 \rightarrow 10^\ddagger$	35.5

*minus first two events (electron scattering)

**minus last three events

†corrected for dead time

‡corrected for σ_{ν_e} deviating from E_ν^2 at low energies

Table 5: Temperatures and Total Energies						
Detector	E_c ($E_0 = E_c + 1.8$)	Effective Events	$\langle E_{\nu_e} \rangle$ ($E_{e^+} + 1.8$)	Effective T_{ν_e}	ϵ_{ν_e} ($\times 10^{52} \text{ergs}$)	ϵ_{total} ($\times 10^{53} \text{ergs}$)
Kamioka	6	16.5	15.4	2.8	7.3	4.8
Kamioka*	6	14.3	14.8	2.7	6.9	4.6
Kamioka	7.5	16.5	15.4	2.6	9.5	6.3
Kamioka*	7.5	14.3	14.8	2.4	9.8	6.5
Kamioka	10	7.8	21.1	3.7	3.0	2.0
Kamioka*	10	5.6	22.1	3.9	1.9	1.3
Kamioka**	6	11.6	17.0	3.2	4.2	2.8
Kamioka†	6	20.5	14.4	2.6	9.5	5.1
IMB‡	18	22	29.2	4.6	4.0	2.6
IMB‡	20	22	29.2	4.1	6.5	4.3
IMB‡	29	10	36.8	4.0	10.0	6.7

*minus first two events

**minus last three events

†corrected for cross section decrease at low E_ν relative to E_ν^2

‡for IMB $Q = 1.3$ MeV instead of 1.8 MeV